Electronic Supplementary Information

Emergence through delicate balance between the steric factor and the molecular orientation: a highly bright and photostable DNA marker for real-time monitoring of cell growth dynamics

Content

Instruments: ^{1}H and ^{13}C NMR spectra were recorded on Jeol JNM ECX 500 MHz spectrometer in $CDCl_3$, CD_3OD and DMSO-d_6. FT-IR spectra were recorded on a Carry-660 FT-IR spectrometer. HRMS-ESI spectra were recorded on Bruker Maxis Impact HD instrument. Using Stuart Melting point apparatus melting points of the solid compounds were recorded. Absorption/Emission spectra were recorded on Simadzu UV-2450 and Cary Eclipse spectrophotometer respectively, using 1 cm quartz cell with 5/5 slit widths. Lifetime and anisotropy measurements were carried out using Fluorescence Lifetime Spectrometer (Agilent technology). The cell imaging experiments were performed employing inverted fluorescent microscope (Nikon Eclipse TS100). FACS analysis was performed in flow cytometer (BD FACS Canto)

Materials: Solvents and chemicals were purchased from commercial resources and directly used without purification. Spectroscopic dimethyl sulfoxide (DMSO) was used for photophysical studies. Doubly ionized water used in all experiments is from Milli-Q systems. PBS (pH = 7.34, 0.1 M, 10x) was prepared using doubly ionized water. DNA (Herring Sperm, Sigma Aldrich) and RNA (Torula yeast, HiMedia lab) solutions (1 mg/mL) were prepared in PBS. Stock solutions of 5 mM for each probe were prepared in DMSO and the aliquots of DNA stock solutions (0 - 38 eq) were incubated with 10 μM solution of each probe for absorption and emission experiments. DNA concentration was determined using absorption maxima at 260 nm by following Jose Portugal et al.[1]

DFT Calculations: The geometry of the probes **RF1-RF3** was optimized by density functional theory (DFT) with B3LYP/6-31G (d, p) basis set [2, 3] with no symmetry constraint using Gaussian 09 suite of programmes.[4] Frequency calculation at the same level with the same basis set was performed to ensure that the geometries correspond to real minima. Gauss view software along with Chemcraft software was used for visualization purpose.[5]

Stoichiometry and dissociation constant Calculation: The binding stoichiometry was determined by Jobs plot and further supported by Hill plot. [6, 7]Emission spectra were recorded by

titrating 0 – 1 mg/mL of DNA against 10 μM of the probes **RF1**-**RF3**. The binding constant values of the probes **RF1**-**RF3** were calculated employing Benesi-Hildebrand equation.[8]

Determination of the experimental limit of detection: Experimental limit of detection was calculated using the reported procedure.[9, 10] DNA concentration at which emission enhancement for the probes was more than 10% of their initial emission intensity was considered as detection limit.

Quantum yield calculation: Quantum yield of the probes **RF1**-**RF3** was determined using Rhodamine 6G (ϕ_R = 0.95, in ethanol) as the standard (on SHIMADZU UV-2450 spectrophotometer and Cary Eclipse spectro photometer, slit widths of excitation and emission are 5/5 respectively) using equation:

$$\phi_S = \phi_R \left(\frac{A_R}{A_S} \right) \left(\frac{D_S}{D_R} \right) \left[\frac{n_S}{n_R} \right]^2$$

Where ϕ_S and ϕ_R; the quantum yields of sample and the reference, A_S and A_R; absorbance of the sample and the reference. D_S and D_R; the areas of emission while n_S and n_R; the refractive indices of the sample and reference solutions respectively.

Extinction coefficient calculation: The extinction coefficients were evaluated for probes **RF1**-**RF3** through the measurement of absorption maxima of the probes 0 – 10 μM using 3 mL of phosphate buffer saline (PBS) and the value of the extinction coefficient was evaluated as the slope of the plot between absorption maxima versus concentrations. [11, 12]Similarly, the absorption spectra of the probes **RF1**-**RF3** were recorded by titrating their various concentration (0 – 10 μM) against 0-38 equivalent of DNA solution and from the slope of absorbance versus concentrations graph extinction coefficients were calculated.

Lifetime measurements: Lifetime measurements were carried out under physiological conditions (PBS, 0.1 M, pH = 7.34) used for previous photophysical studies. Fluorescence Lifetime Spectrometer (Agilent technology) using 560 nm light emitting diode (LED) was employed to evaluate the excited state dynamics.

Cell culture: HeLa cells were used for cell based fluorescence characterization of probes. Cell line was procured from National Centre for Cell Science, India. Cells cultured in α-MEM culture media containing L-glutamine and non-essential amino acids and supplemented with 10 % Fetal

Bovine Serum was used. Antibiotic cocktail penicillin, streptomycin and amphotericin B were used to get rid of any contaminants. Cells were maintained in 5 % CO_2 and 95 % air atmosphere at 37°C with 80 % humidity. Culture media was changed every third day.

MTT assay: For cytotoxicity testing, 5×10^3 cells HeLa cells were seeded per well of 96 well plate and cultured for 24 h. Next day, cells were treated with **RF1** at 10 μM concentrations for duration of 24 h at 37°C, 5% CO_2 atmosphere. MTT (3-5 mg/mL) was added 4 h before the completion of incubation period for measuring cytotoxicity of the probes **RF1**.[13] DMSO was added to lyse the cells and dissolve the formed formazan crystals. Wavelength of 565 nm was used as measurement wavelength by taking 630 nm as reference control (Tecan, M7500 pro) for optical density measurement. Cell viability was measured with respect to untreated control.

Photobleaching resistance: The photostability of the probe **RF1** was quantified in terms of their half-life time in solution assay. For this experiment under continuous illumination of Hg-vapor lamp (160 W, 2.1×10^3 Lux) sample was exposed in a closed chamber. Similarly, the fixed cells were stained with **RF1** (10 μM) and continuously exposed to PI channel using fluorescent microscope (Nikon Eclipse TS100) for duration of 10 min to get the photostability in cellular medium. Additionally, the photostability of **RF1** in the cellular medium was compared with Ethidium bromide, DAPI, and Syto-16 using a set of LEDs (LED microscope EVOS FL auto imager, Applied biosystems) for the visible light irradiation at their own excitation wavelength (RFP, DAPI, and GFP channel respectively). Fluorescence/photo bleaching was measured using Image J software. The fluorescence at 0 min was considered as 100% and fluorescence retention in each case was calculated by taking this value as reference control.

Phototoxicity assay: 5×10^3 cells were incubated per well of 96-well plates with 10 μM of **RF1** for 24 h at 37°C. Next day, a continuous exposure of LED light was given per well for 5 min in triplicates under RFP channel of LED microscope (EVOS FL auto imager). Cells without probe were also exposed for same duration of light and used as control. Cells were further incubated at 37°C for 6 h and phototoxicity was measured by MTT assay.

Monitoring of cellular growth: 5×10^3 HeLa cells were seeded per well of a six-well plate in triplicates for each probe. Single cell suspension was incubated with RF1 at 10 μM concentration for 2 h. Cells were washed twice with culture media and incubated in 37°C/5% CO2 incubator

in MEM media supplemented with 10% FBS. Media was changed every third day and cells were photographed every day. Cells were visualized under fluorescent microscope (Nikon TS100) at PI filter with excitation wavelength 536 nm and emission wavelength of 617 nm. Quantitation of mean fluorescent intensity was done using image J by measuring fluorescent intensity of at least ten cells per photograph. FACS analysis was performed on trypsinized cells at 9th day in flow cytometer (BD FACS Canto) and statistics of fluorescence were recorded. Cells stained for 2 h were taken as control.

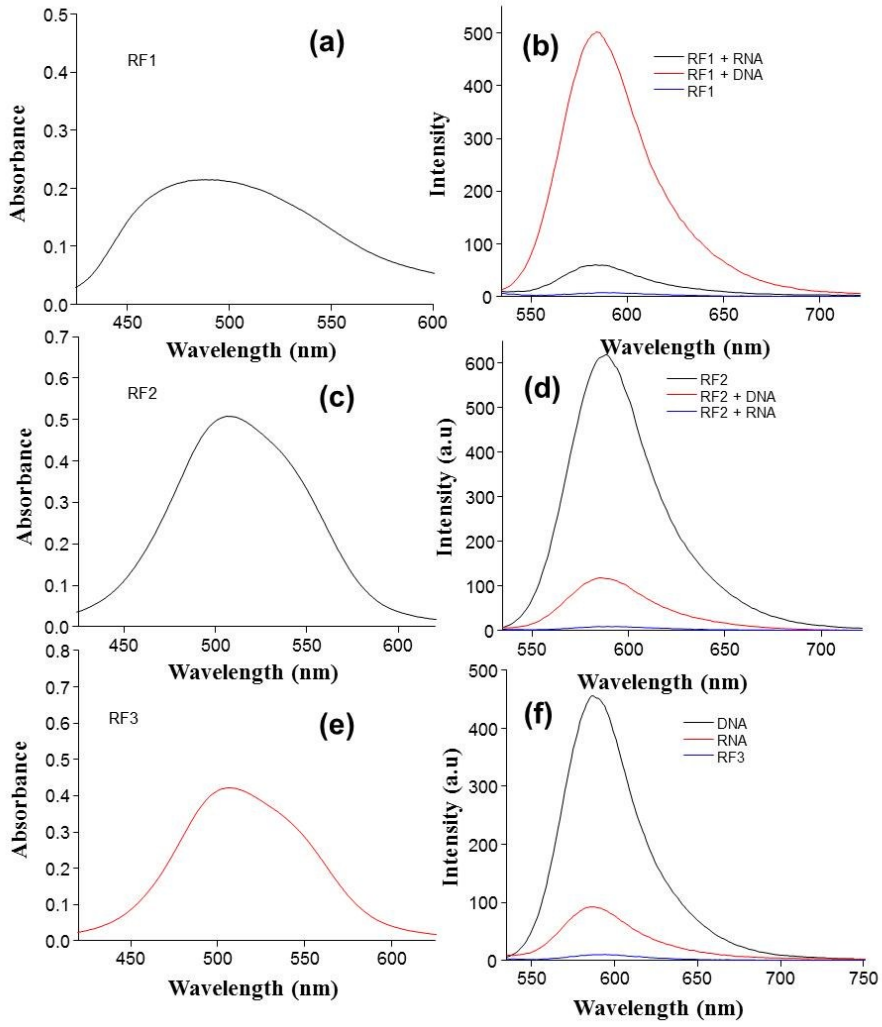

Fig. S1: The optical responses of the probes (**RF1-RF3**). a, c, e) Absorption maxima and b, d, f) emission spectra of **RF1-RF3** respectively. The optical behaviour was studied under physiological conditions (PBS, 0.1 M, pH = 7.34) using 10 µM as the probes concentration and 1 mg/mL DNA/RNA.

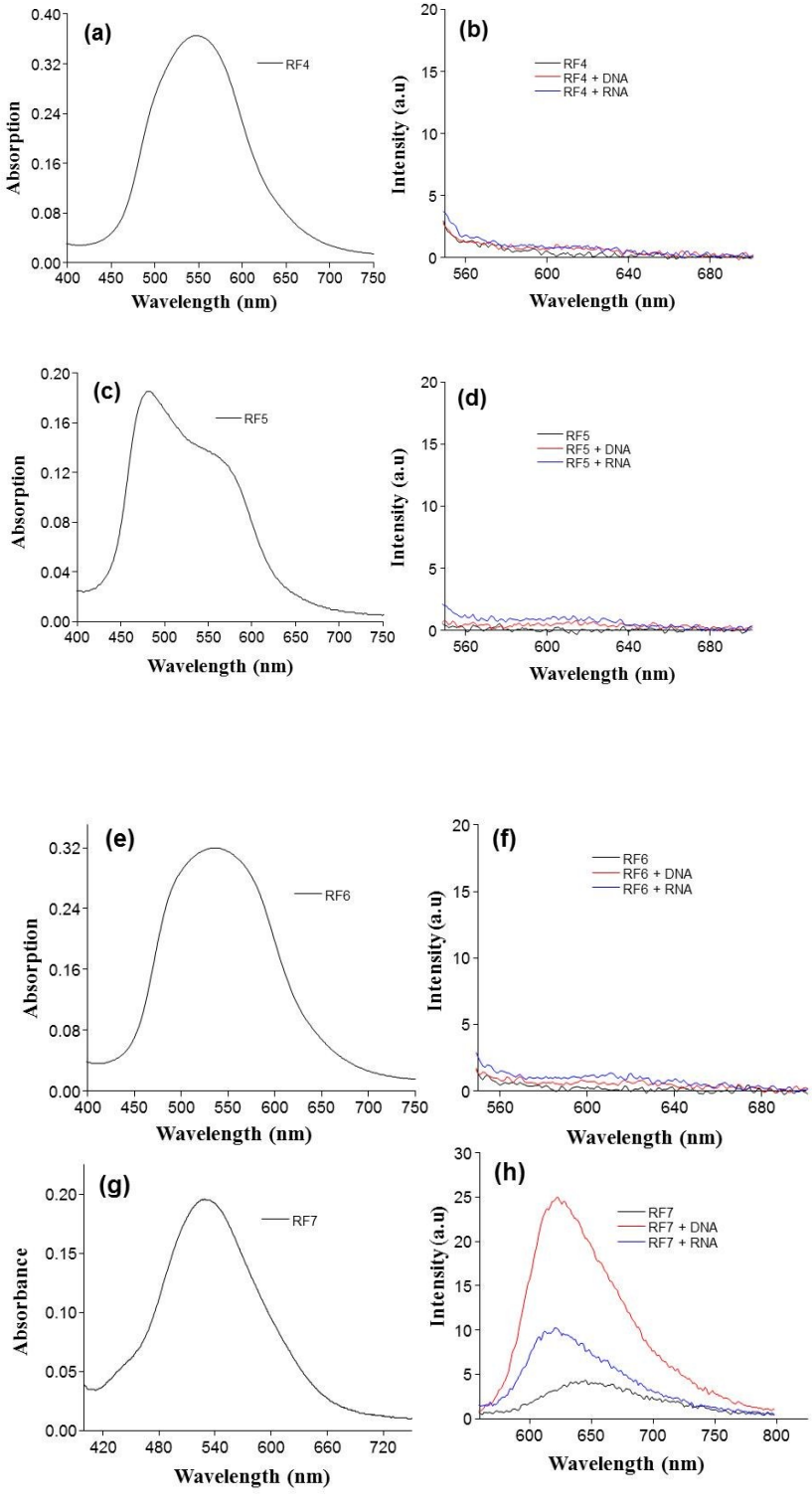
(a)
RF4
Absorption
Wavelength (nm)
(b)
RF4
RF4 + DNA
RF4 + RNA
Intensity (a.u)
Wavelength (nm)
(c)
RF5
Absorption
Wavelength (nm)
(d)
RF5
RF5 + DNA
RF5 + RNA
Intensity (a.u)
Wavelength (nm)
(e)
RF6
Absorption
Wavelength (nm)
(f)
RF6
RF6 + DNA
RF6 + RNA
Intensity (a.u)
Wavelength (nm)
(g)
RF7
Absorbance
Wavelength (nm)
(h)
RF7
RF7 + DNA
RF7 + RNA
Intensity (a.u)
Wavelength (nm)

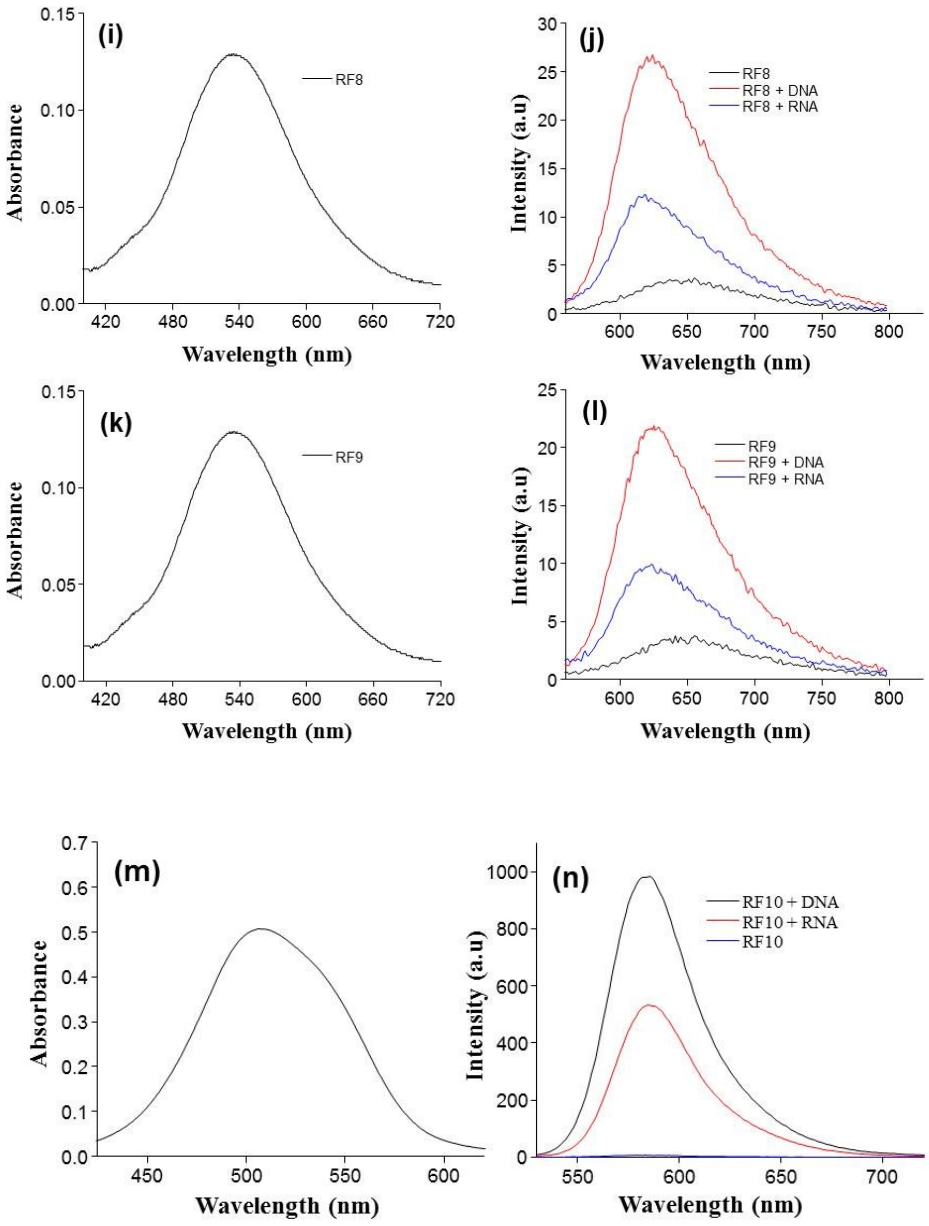

Fig. S2: The optical responses of the probes (**RF4-RF10**). a, c, e, g, i, k, m) Absorption maxima and b, d, f, h, j, l, n) emission spectra of **RF4-RF10** respectively. The optical behaviour was studied under physiological conditions (PBS, 0.1 M, pH = 7.34) using 10 μM as the probes concentration and 1 mg/mL DNA/RNA.

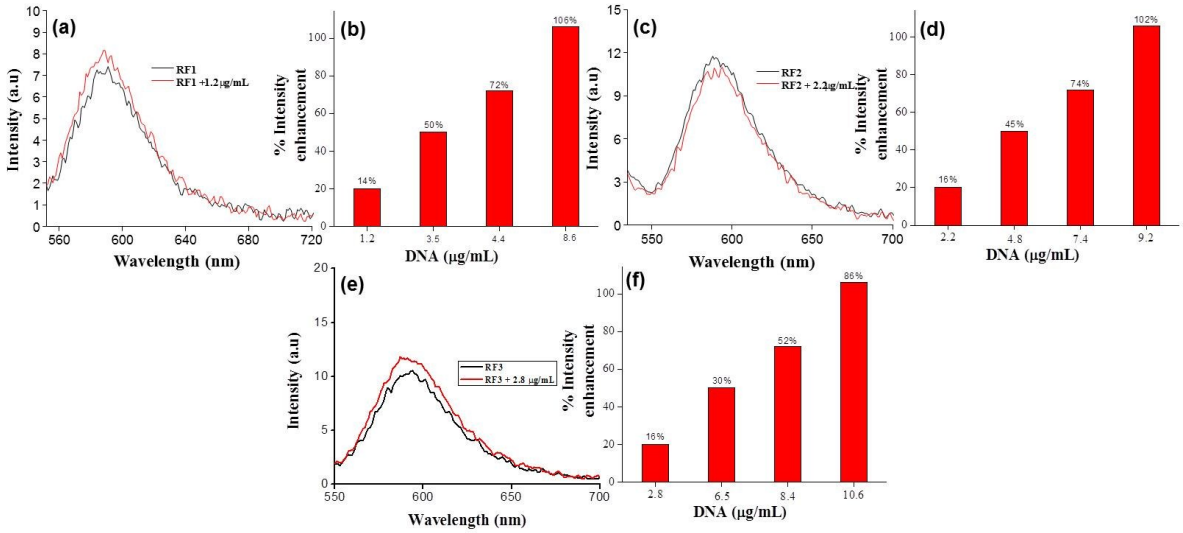

Fig. S3: Calculation of experimental limit of detection of **RF1-RF3.**

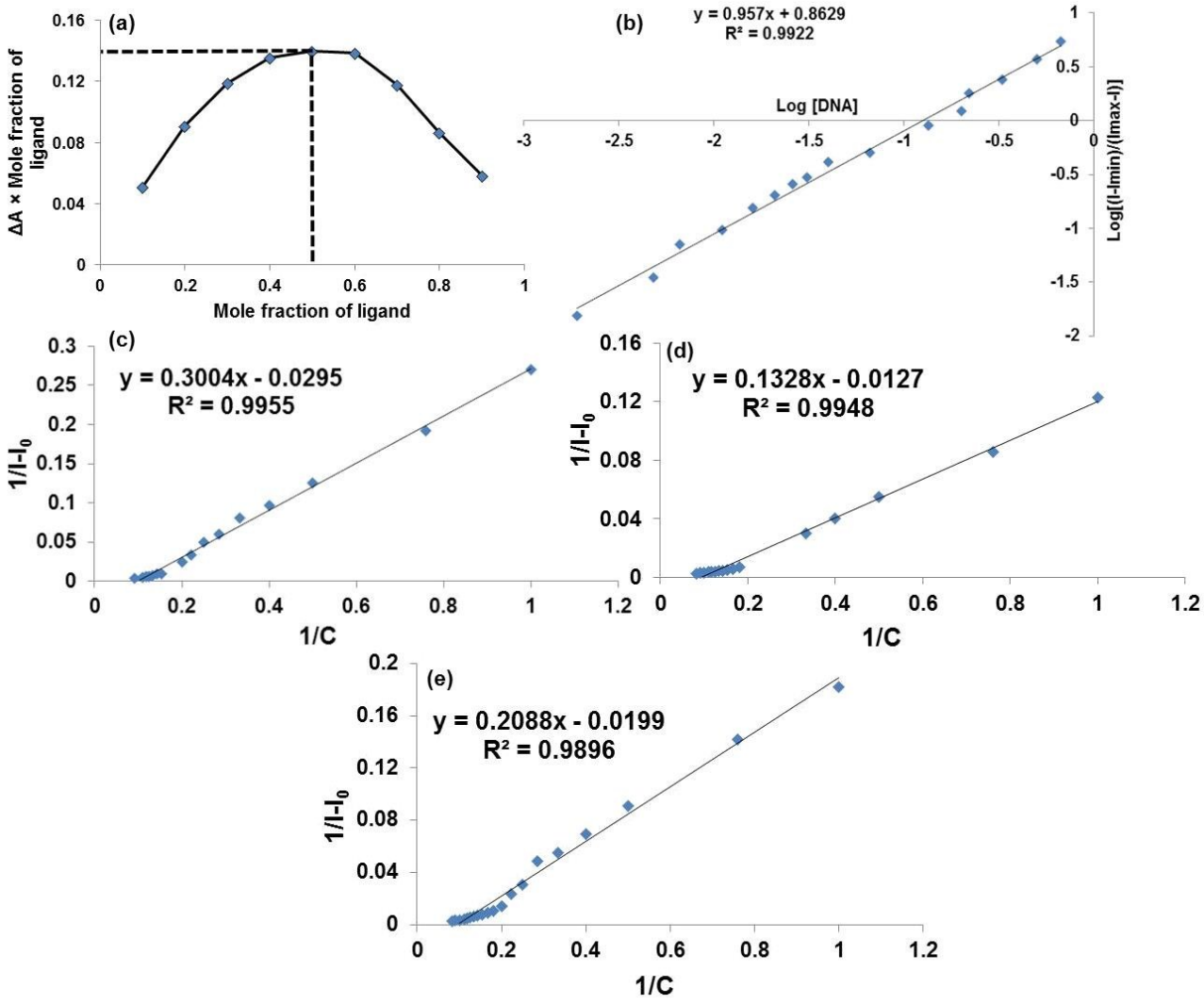

Fig. S4: a**)** Jobs plot; b) Hill plot (m = 1) showing Binding stoichiometry (1:1); c, d, e) Calculation of binding constant of **RF1-RF3.**

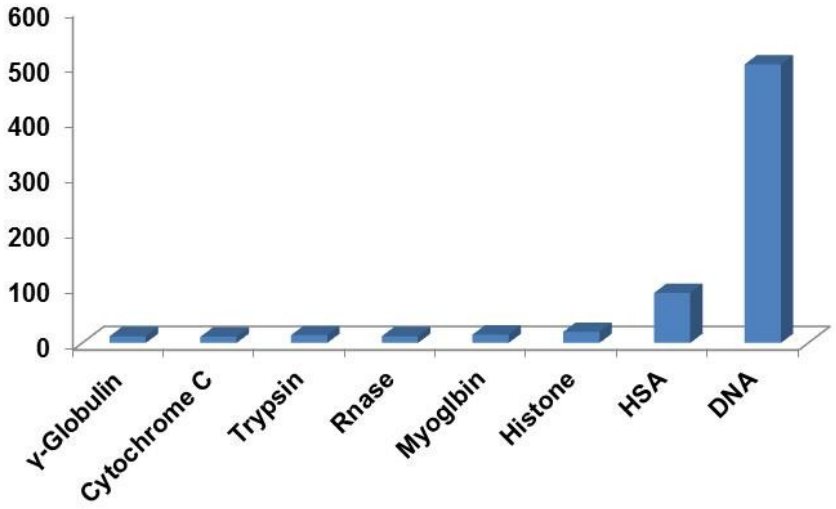

Fig. S5: Measurement of selectivity of **RF1** towards DNA as compared to other competitive biomolecules.

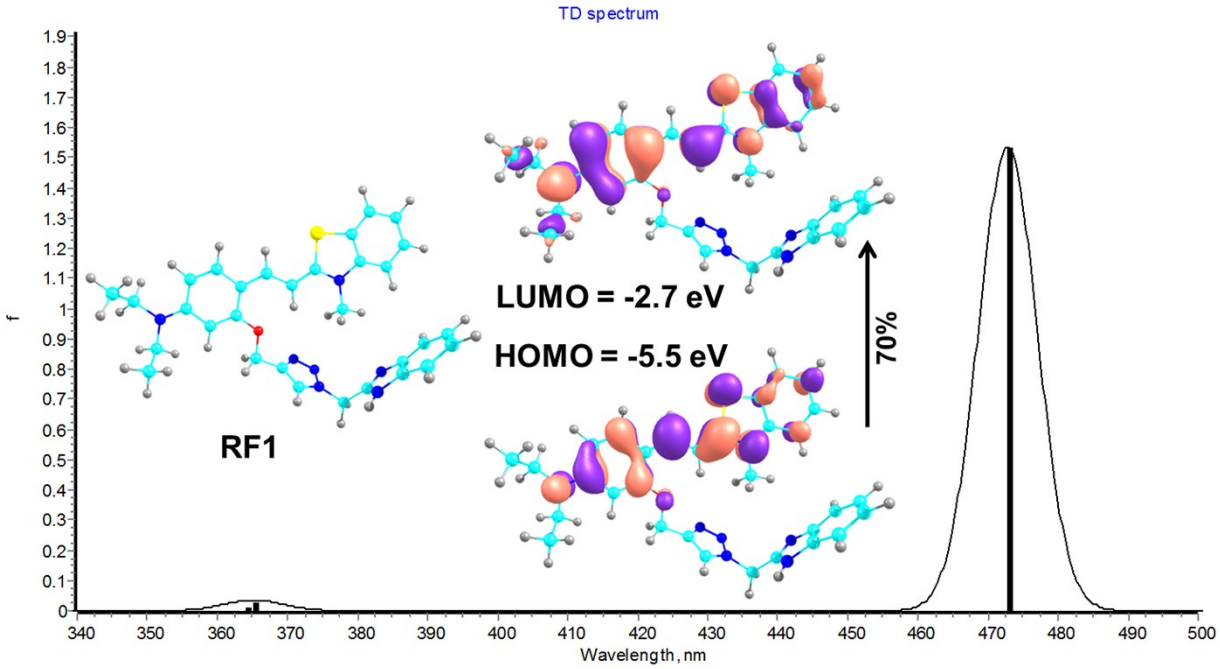

Fig. S6: Showing the outcomes molecular simulation including optimized geometry, corresponding HOMOs-LUMOs and UV-spectra of **RF1.**

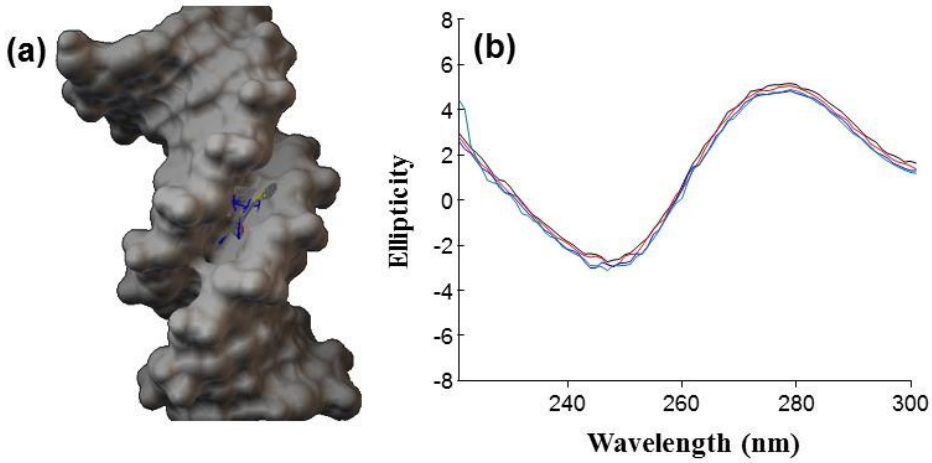

Fig. S7: a, b) Theoretically optimized geometry of **RF1**-DNA complex and CD-spectra of **RF1** (0-10 μM) in the presence of DNA (1 mg/mL).

Probe	Ex/Em (nm)	Extinction coefficient (ϵ) $M^{-1}cm^{-1}$	Quantum yield (ϕ)	Brightness B = (ϕ × ϵ)	Stokes shift (nm)	Detection Limit (μg/mL)	Binding constant (M^{-1})
RF1 + DNA	490/585	52600	0.5	26300	95	1.2	9.8×10^4
RF2 + DNA	520/588	54600	0.7	40400	68	2.2	9.5×10^4
RF3 + DNA	520/587	45600	0.5	26904	67	2.8	9.5×10^4

Table S1: Photophysical parameters of the probes **RF1-RF3** in the presence of DNA.

	RF1 + DNA	RF4 + DNA	RF7 + DNA	RF1 + Glycerol
τ_{av} (ns)	2.6	0.17	0.47	0.9
χ^2	1.17	1.19	1.18	1.15

Table S2: Lifetime measurement of the probes **RF1**, **RF4** and **RF7** (10 μM) in the presence of DNA (1 mg/mL) and **RF1** in glycerol using 560 nm LED.

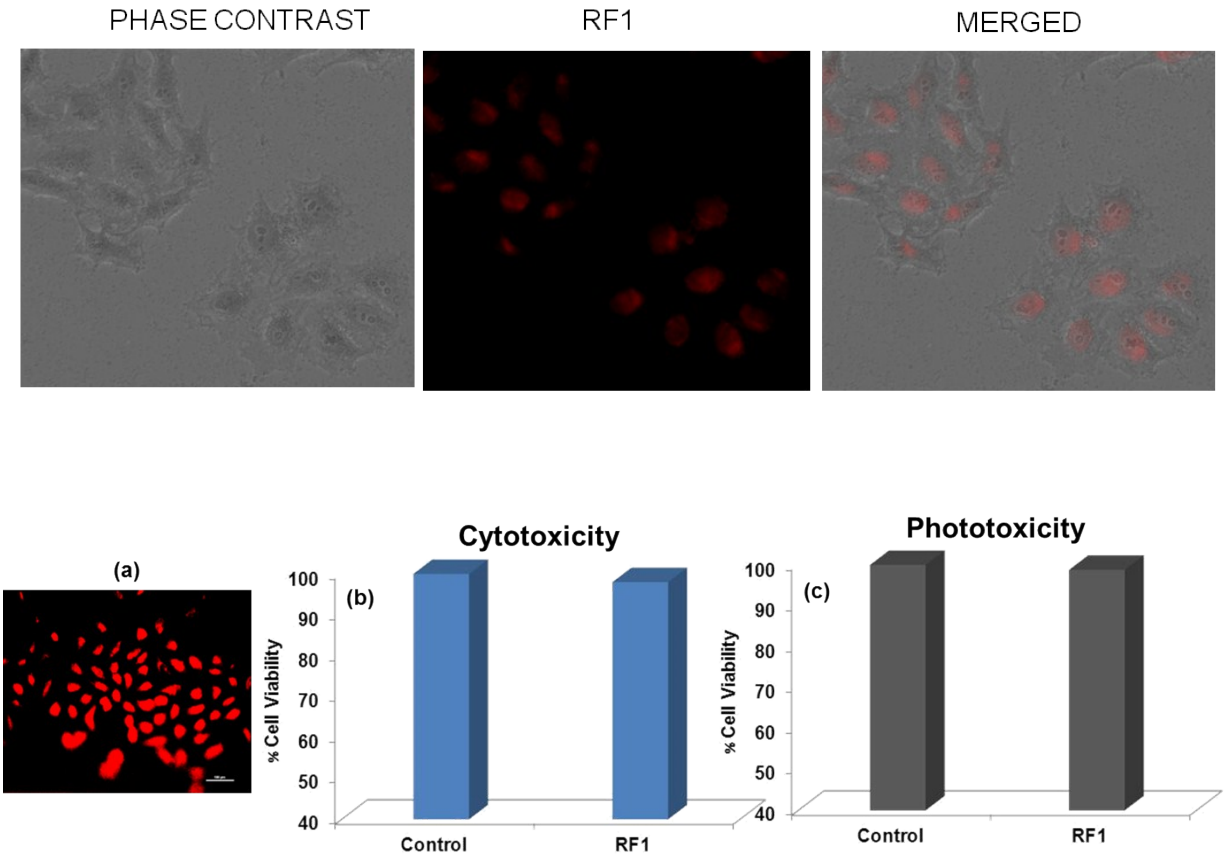

Fig. S8: a) Live HeLa cells stained with **RF1** at 10µM concentration; b, c) showing the quantification of cytotoxicity and phototoxicity of **RF1** (10 µM) in HeLa cells respectively.

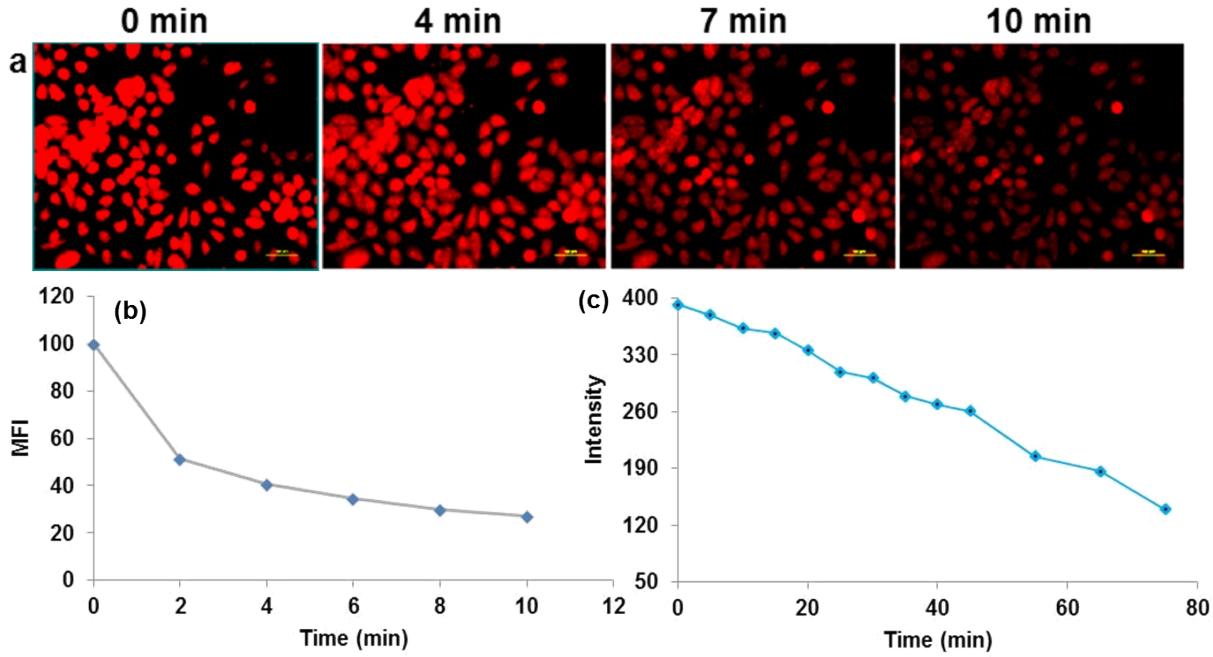

Fig. S9: **Quantification of Photostability in cell and solution:** a) and b) showing the decrease in the fluorescence intensity of **RF1** in cellular medium with respect to time upon continuous exposure of PI channel, c) showing the decrease in the fluorescence intensity of **RF1** in solution under mercury vapour lamp (160 W, 2.1×10^3 Lux). The measured half-life time ($t_{1/2}$) was found >57 min.

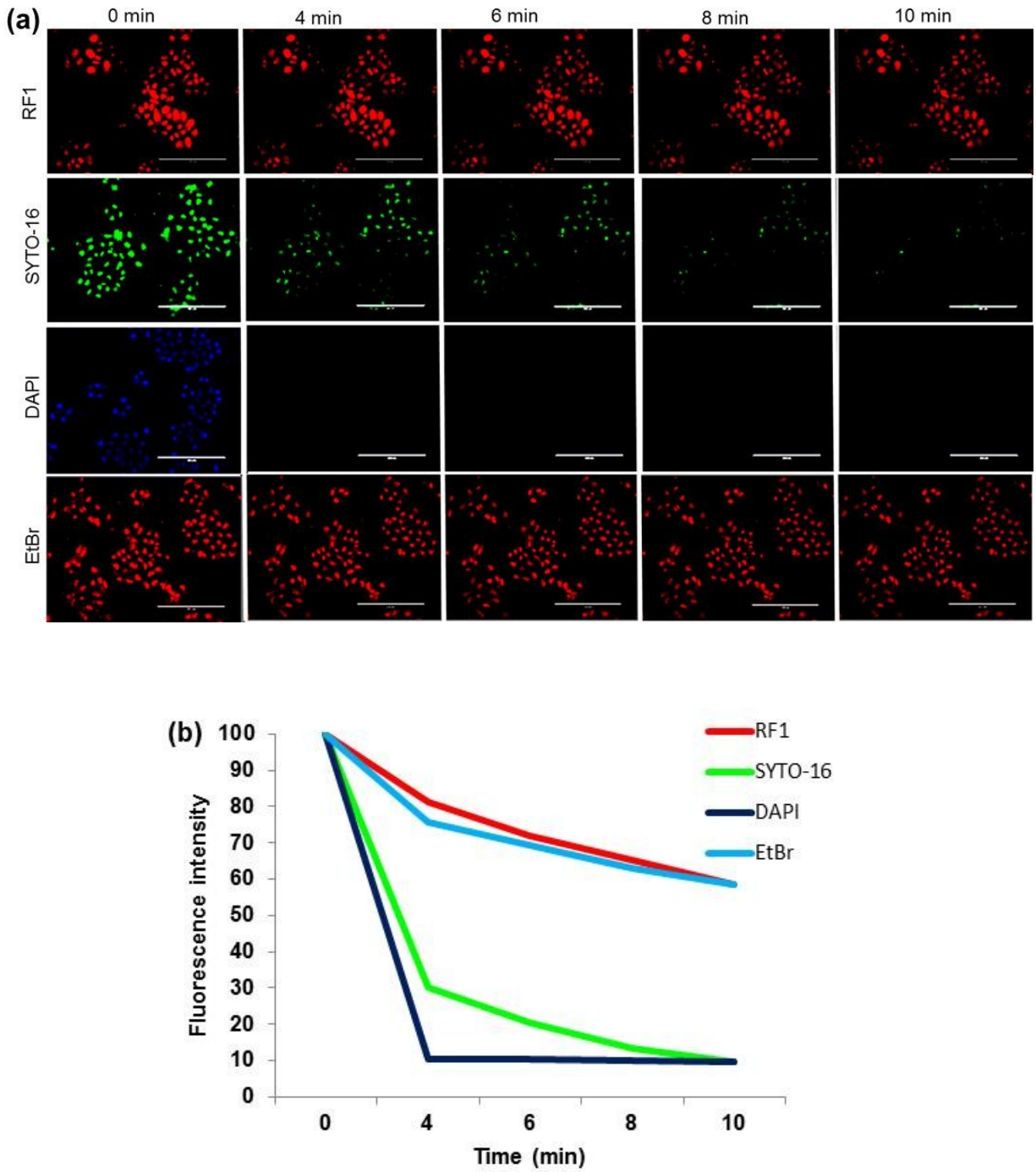

Fig. S10: a, b) Photostability comparison of **RF1** with Syto-16, DAPI and Ethidium bromide in cellular system for 10 min under continuous exposure of a set of LEDs at their own excitation wavelength. Scale bar-200µm.

Synthesis and Characterization:

Azoles (HA1-HA3) and azides (AZ1-AZ3): The azoles were synthesized by following the reported methods [14] and their corresponding azides were synthesized by stirring the mixture of azoles and azide in DMSO at room temperature for overnight.

1) **Derivatives of Thiazole (P1-P3):** 2-methyl benzolthiazole as a greenish liquid was synthesized by following the reported method.[15] Then, nitro derivative of 2-methyl benzolthiazole was obtained as a light brown solid and further the nitro was reduced to amine to accomplish the synthesis of amino derivative of the thiazole (1eq of 2-methyl-5-nitro benzolthiazole, 10 eq of iron and 4 eq of hydrochloric acid were heated to reflux in ethanol-water mixture, 3:2 for 24 h).[16] Next, the alkyl derivative (**P3**) of 5-amino-2-methyl benzothiazole was synthesized as yellowish liquid by stirring the mixture of amine (1 eq), ethyl bromide (2.5 eq) and potassium carbonate (3 eq) in dimethyl formamide (DMF, 2 mL/mmol) at room temperature for 24 h and followed by extraction using dichloromethane-ice cold water mixture.[17]
2) **Iodide salts of thiazole (S1-S3):** The iodide salts of **P3** was obtained by stirring the mixture of **P3** (1eq) and methyl iodide (1.5 eq) in dichloromethane at room temperature for 12 h and followed by the washing of green precipitates by diethyl ether 2-3 times. Whereas the thiazolium salts **S1/S2** were obtained by refluxing **P1/P2** (1 eq) and methyl iodide (1.5 eq) in acetonitrile (3 mL/mmol) for 12 h in the form of white and green solid respectively by washing with ethyl acetate 2-3 times.[18]
3) **Compounds B1 & B2:** 2-hydroxy-4-diethylamino benzaldehyde (1 eq), alkyl bromide (1.2 eq) and potassium carbonate (2 eq) were mixed in dimethyl formamide (DMF, 1.5 mL/mmol) and stirred at room temperature for 12 h. The progress of the reaction was monitored using thin layer chromatography. The mixture was poured on ice cubes and the brown colored precipitates were filtered and washed with cold water. The product was dried and washed with diethyl ether to get pure product.
4) **Triazoles (T1-T3):** The triazoles **T1-T3** were synthesized from the **B1** (1eq) and the corresponding azides (1.2 eq) by adding freshly prepared solution of $CuSO_4.5H_2O$ (10 mol %) and sodium ascorbate (30 mol %) in a mixture of t-butanol/water/THF (3 mL/mmol, 1:1:1). The resulting mixture was stirred at room temperature for overnight.

The progress of the reaction was monitored by thin layer chromatography. On completion, the products were extracted with dichloromethane (DCM) with 2-3 times and washed with diethyl ether. Further, the recrystallization using ethanol gave the pure products.

5) **Probes (RF1-RF10):** The probes were synthesized from their corresponding precursors by Knovenangel condensation by refluxing the aldehydes (1eq) and the thiazolium salts (0.91 eq) in ethanol (3 mL/mmol). The colored precipitates were filtered and washed with ethyl acetate for 3-4 times to get the pure products.[19]

P3: Rf = 71%, Brown liquid, Yield: 40%, FT-IR (ν in cm^{-1}): 2980, 1585, 1530, 1475. ^{1}H NMR (500 MHz, $CDCl_3$): δ = 7.65 (d, J = 8.95 Hz, 1H), 6.91 (s, 1H), 6.76-6.74 (m, 1H), 3.31-3.27 (q, J = 6.9 Hz, 4H), 2.64 (s, 3H), 1.08 (t, J = 5 Hz, 6H) ppm. ^{13}C NMR (125 MHz, $CDCl_3$): 161.2, 145.7, 144.5, 137.8, 122.3, 102.4, 44.8, 19.7, 12.4 ppm. HRMS: *m/z* calculated for $C_{12}H_{16}N_2S$ [M + H] 221.1112, found 221.1106.

S2: Rf = 52%, Greenish solid, Yield: 75%, M.P. - 220^0C, FT-IR (ν in cm^{-1}): 2975, 1597, 1537, 1493, 1357, 1286. ^{1}H NMR (500 MHz, DMSO-d_6): δ = 9.45 (s, 1H), 8.68-8.65 (s, 1H), 8.53-8.51 (s, 1H), 4.2 (s, 3H), 3.2 (s, 3H) ppm. ^{13}C NMR (125 MHz, DMSO-d_6): 183, 146, 145, 129.6, 124.16, 121, 118, 36.9, 18 ppm. HRMS: *m/z* calculated for $C9H9N_2O_2S$ [M - I] 209.0385, found 209.0379.

S3: Rf = 52%, Greenish solid, Yield: 78%, M.P. - 106.0^0C FT-IR (ν in cm^{-1}): 2975, 1597, 1537, 1493, 1357, 1286. ^{1}H NMR (500 MHz, DMSO-d_6): δ = 7.96 (d, J = 9.65 Hz, 1H), 7.52 (s, 1H), 7.19-7.16 (m, 1H), 4.9 (s, 3H), 3.46-3.42 (q, J = 7.6 Hz, 4H), 3.0 (s, 3H), 1.13 (t, J = 6.85 Hz, 6H) ppm. ^{13}C NMR (125 MHz, DMSO-d_6): 169.4, 147.3, 131.8, 131.1, 117.1, 114.2, 103, 79, 44.2, 35.5, 16.4, 12.2 ppm. HRMS: *m/z* calculated for $C_{13}H_{19}N_2S$ [M - I] 235.1269, found 235.1263.

T1: Rf = 57%, Yellow solid, Yield: 58%, M.P. - 173^0C, FT-IR (ν in cm^{-1}): 2976, 1648, 1584, 1520, 1394, 1265, 1109. ^{1}H NMR (500 MHz, $CDCl_3$): δ = 9.93 (s, 1H), 7.9 (s, 1H), 7.62-7.53 (m, 3H), 7.20-7.19 (m, 2H), 6.24-6.22 (m, 1H), 5.85 (s, 2H), 5.1 (s, 2H), 3.36-3.32 (m, 4H), 1.14 (t, J = 6.9 Hz, 6H) ppm. ^{13}C NMR (125 MHz, $CDCl_3$): 187.2, 162.6, 153.9, 144, 131.2, 124.1,

113.9, 104.8, 93.9, 62, 44.7, 12.44 ppm. HRMS: *m/z* calculated for $C_{22}H_{24}N_6O_2$ [M + H] 405.2039, found 405.2031.

T2: Rf = 61%, Brown solid, Yield: 72%, M.P. - 154^{0}C, FT-IR (ν in cm^{-1}): 2972, 1640, 1582, 1518, 1392, 1262, 1115. ^{1}H NMR (500 MHz, $CDCl_3$): δ = 10 (s, 1H), 7.9 (s, 1H), 7.75-7.73 (m, 1H), 7.69-7.68 (m, 1H), 7.54-7.53 (m, 1H), 7.40-7.37 (m, 3H), 6.30-6.28 (m, 1H), 6.25-6.24 (m, 1H), 5.87 (s, 2H), 5.35 (s, 2H), 3.43-3.39 (m, 4H), 1.19 (t, J = 7.6 Hz, 6H) ppm. ^{13}C NMR (125 MHz, $CDCl_3$): 186.8, 162.5, 158.3, 153.8, 150.9, 144.9, 131.0, 126.2, 125, 123.6, 114.1, 111, 104.7, 93.9, 62.3, 47.2, 44.8, 12.5 ppm. HRMS: *m/z* calculated for $C_{22}H_{23}N_5O_3$ [M + H] 406.1879, found 406.1873.

T3: Rf = 62%, Yellow solid, Yield: 72%, M.P. – 126.5^{0}C, FT-IR (ν in cm^{-1}): 2971, 1642, 1590, 1510, 1385, 1261, 1102. ^{1}H NMR (500 MHz, $CDCl_3$): δ = 10 (s, 1H), 8.05-8.03 (m, 1H), 7.93 (s, 1H), 7.87-7.85 (m, 1H), 7.68-7.66 (m, 1H), 7.53-7.50 (m, 1H), 7.44-7.41 (m, 1H), 6.29-6.27 (m, 1H), 6.23 (s, 1H), 5.98 (s, 2H), 5.33 (s, 2H), 3.42-3.38 (m, 4H), 1.18 (t, J = 6.85 Hz, 6H) ppm. ^{13}C NMR (125 MHz, $CDCl_3$): 186.8, 162.5, 158.3, 153.8, 150.9, 144.9, 131.0, 126.2, 125, 123.6, 114.1, 111, 104.7, 93.9, 62.3, 47.2, 44.8, 12.5 ppm. HRMS: *m/z* calculated for $C_{22}H_{23}N_5O_2S$ [M + H] 422.1651, found 422.1645.

RF1: Rf = 51%, Dark red solid, Yield: 52%, M.P. - 227.5^{0}C, FT-IR (ν in cm^{-1}): 3078, 1613, 1567, 1516, 1399, 1343, 1263, 1199. ^{1}H NMR (500 MHz, DMSO-d_6): δ = 8.47 (s, 1H), 8.16 (d, J = 8.25 Hz, 1H), 8.0-7.97 (m, 1H), 7.86-7.84 (m, 1H), 7.97-7.77 (m, 1H), 7.71-7.69 (m, 1H), 7.62-7.59 (m, 1H), 7.56-7.53 (m, 3H), 7.22-7.19 (m, 1H), 7.16-7.12 (m, 1H) 6.52-6.49 (m, 2H), 5.95 (s, 2H), 5.4 (s, 2H), 3.8 (s, 3H), 3.55-3.51 (m, 4H), 1.16 (t, J = 6.9 Hz, 6H) ppm. ^{13}C NMR (125 MHz, DMSO-d_6): 171.14, 161.2, 153.5, 148.35, 142.42, 141.8, 128.65, 127.1, 126.2, 125.51, 123.62, 122.76, 121.67, 118.88, 115.42, 111.68, 111.11, 106.13, 105.3, 94.8, 61.7, 47.4, 44.5, 34.8, 12.6 ppm. HRMS: *m/z* calculated for $C_{32}H_{32}N_7OS$ [M - I] 550.2389, found 550.2350.

RF2: Rf = 52%, Violet solid, Yield: 52%, M.P. - 190.0^{0}C, FT-IR (ν in cm^{-1}): 3075, 1615, 1562, 1512, 1405, 1350, 1275, 1210. ^{1}H NMR (500 MHz, DMSO-d_6): δ = 8.56 (s, 1H), 8.17-8.16 (m, 1H), 8.02-7.99 (m, 1H), 7.96-7.94 (m, 1H), 7.81-7.80 (m, 1H), 7.74-7.70 (m, 3H), 7.63-7.54 (m, 2H), 7.43-7.36 (m, 2H), 6.54-6.51 (m, 2H), 6.18 (s, 2H), 5.47 (s, 2H), 3.98 (s, 3H), 3.56-3.52 (m,

4H), 1.17 (t, J = 6.8 Hz, 6H) ppm. ^{13}C NMR (125 MHz, DMSO-d_6): 171.2, 161.1, 160.5, 153.6, 150.3, 142.6, 141.9, 140.1, 128.7, 127, 126.2, 125.9, 124.9, 119.9, 115.4, 111.1, 106.1, 105.3, 94.8, 61.6, 46.7, 44.5, 34.9, 12.6 ppm. HRMS: *m/z* calculated for $C_{31}H_{31}N_6O_2S$ [M - I] 551.2229, found 551.2258.

RF3: Rf = 54%, Violet solid, Yield: 52%, M.P. - 145.0^{0}C, FT-IR (ν in cm^{-1}): 3070, 1620, 1557, 1525, 1415, 1360, 1245. ^{1}H NMR (500 MHz, DMSO-d_6): δ = 8.58 (s, 1H), 8.13-8.08 (m, 2H), 7.97-7.91 (m, 2H), 7.87-7.85 (m, 1H), 7.76-7.74 (m, 1H), 7.68-7.55 (m, 1H), 7.51-7.43 (m, 1H), 6.46-6.42 (m, 2H), 6.28 (s, 2H), 5.44 (s, 2H), 3.91 (s, 3H), 3.51-3.47 (m, 4H), 1.16 (t, J = 6.85 Hz, 6H) ppm. ^{13}C NMR (125 MHz, DMSO-d_6): 170.9, 165.2, 160.9, 153.5, 152.2, 142.7, 141.8, 134.9, 128.6, 126.9, 126.6, 126.2, 125.7, 123.5, 122.8, 115.3, 111.2, 106.1, 105.2, 94.8, 61.8, 50.8, 44.5, 34.9, 12.6 ppm. HRMS: *m/z* calculated for $C_{31}H_{31}N_6OS_2$ [M - I] 567.2001, found 567.2001.

RF4: Rf = 48%, Violet solid, Yield: 55%, M.P. - 223.0^{0}C, FT-IR (ν in cm^{-1}): 3064, 1616, 1564, 1475, 1453, 1255, 1186. ^{1}H NMR (500 MHz, DMSO-d_6): δ = 12.76 (s, 1H), 9.0 (s, 1H), 8.52 (s, 1H), 8.40-8.38 (m, 1H), 7.95-7.89 (m, 2H), 7.37-7.36 (s, 1H), 7.54 (s, 2H), 7.39-7.37 (m, 1H), 7.19-7.16 (m, 3H), 6.5-6.4 (m, 2H), 5.99 (s, 2H), 5.43 (s, 2H), 3.83 (s, 3H), 3.54-3.52 (m, 4H), 1.17 (t, J = 6.9 Hz, 6H) ppm. ^{13}C NMR (125 MHz, DMSO-d_6): 173.2, 161.8, 154.6, 145.8, 144.6, 142.2, 127.1, 125.6, 123.9, 122.7, 121.6, 119.8, 118.8, 115.2, 112.1, 111.7, 106.9, 94.6, 61.7, 47.5, 44.8, 35, 12.6 ppm. HRMS: *m/z* calculated for $C_{31}H_{31}N_8O_3S$ [M - I] 595.224, found 595.2243.

RF5: Rf = 51%, Violet solid, Yield: 54%, M.P. - 176.0^{0}C, FT-IR (ν in cm^{-1}): 3060, 1610, 1570, 1465, 1443, 1250, 1182. ^{1}H NMR (500 MHz, DMSO-d_6): δ = 9.0 (s, 1H), 8.6 (s, 1H), 8.43-8.40 (m, 1H), 8.01-7.97 (m, 2H), 7.75-7.72 (m, 3H), 7.45-7.38 (m, 3H), 6.53-6.43 (m, 2H), 6.21 (s, 2H), 5.48 (s, 2H), 3.93 (s, 3H), 3.57-3.53 (m, 4H), 1.18 (t, J = 6.9 Hz, 6H) ppm. ^{13}C NMR (125 MHz, DMSO-d_6): 173.2, 160.5, 154.6, 152.8, 150.3, 145.9, 144.7, 142.4, 140.2, 127.1, 126.0, 125.9, 124.9, 123.9, 119.9, 115.4, 112.1, 110, 94.7, 61.8, 46.7, 44.7, 35.2, 12.7 ppm. HRMS: *m/z* calculated for $C_{31}H_{30}N_7O_4S$ [M - I] 596.2080, found 596.2081.

RF6: Rf = 52%, Violet solid, Yield: 52%, M.P. - 190.0^{0}C, FT-IR (ν in cm^{-1}): 3070, 1620, 1565, 1462, 1440, 1252, 1175. ^{1}H NMR (500 MHz, DMSO-d_6): δ = 9.0 (s, 1H), 8.6 (s, 1H), 8.41-8.39 (m, 1H), 8.11-8.09 (m, 1H), 7.97-7.94 (m, 3H), 7.52-7.50 (m, 1H), 7.49-7.40 (m, 2H), 6.52-6.41 (m, 2H), 6.29 (s, 2H), 5.46 (s, 2H), 3.89 (s, 3H), 3.56-3.52 (m, 4H), 1.17 (t, J = 6.9 Hz, 6H) ppm. ^{13}C NMR (125 MHz, DMSO-d_6): 173.1, 165.2, 154.6, 152.2, 145.9, 144.7, 142.4, 134.8, 127.1, 126.6, 125.8, 123.8, 122.8, 119.7, 115.4, 112.1, 94.7, 61.8, 50.83, 44.8, 35.2, 12.7 ppm. HRMS: *m/z* calculated for $C_{31}H_{30}N_7O_3S_2$ [M - I] 612.1852, found 612.1855.

RF7: Rf = 54%, Violet solid, Yield: 35%, M.P. - 247.0^{0}C, FT-IR (ν in cm^{-1}): 3069, 1615, 1565, 1512, 1392, 1334, 1258, 1188. ^{1}H NMR (500 MHz, DMSO-d_6): δ = 8.7 (s, 1H), 7.68-7.66 (m, 2H), 7.35-7.26 (m, 3H), 7.20-7.19 (m, 2H), 7.12-7.10 (m, 1H), 7.04-7.02 (m, 1H), 6.77-6.75 (m, 1H), 6.19 (s, 2H), 6.1 (s, 1H), 5.13 (s, 2H), 3.8 (s, 3H), 3.39-3.32 (m, 8H), 1.22-1.15 (m, 12H) ppm. ^{13}C NMR (125 MHz, DMSO-d_6): 165.6, 163.7, 160.8, 152.7, 147.2, 143, 135.5, 131.6, 129.5, 125.1, 123.3, 121.8, 115, 113.1, 111.6, 105.8, 103.5, 94.5, 62.4, 51.8, 45, 36, 31.5, 29.5, 12.7, 12.4 ppm. HRMS: *m/z* calculated for $C_{35}H_{41}N_8OS$ [M - I] 621.3124, found 621.3118.

RF8: Rf = 51%, Violet solid, Yield: 38%, M.P. - 255.0^{0}C, FT-IR (ν in cm^{-1}): 3065, 1610, 1562, 1382, 1340, 1258, 1175. ^{1}H NMR (500 MHz, DMSO-d_6): δ = 8.5 (s, 1H), 7.79-7.7 (m, 5H), 7.52-7.48 (m, 1H), 7.42-7.35 (m, 4H), 7.07-7.04 (m, 1H), 6.47 (s, 2H), 5.75 (s, 2H), 5.43 (s, 2H), 3.92 (s, 3H), 3.52-3.48 (m, 4H), 3.45-3.40 (m, 4H), 1.17-1.10 (m, 12H) ppm. ^{13}C NMR (125 MHz, DMSO-d_6): 165.4, 160.5, 152.5, 150.4, 147, 131.9, 129.2, 125.9, 124.9, 119.9, 116, 113.5, 111, 105.7, 103.1, 95, 61.6, 54.9, 46.6, 44.2, 35, 29, 12.7, 12.2 ppm. HRMS: *m/z* calculated for $C_{35}H_{40}N_7O_2S$ [M - I] 622.2964, found 622.2958.

RF9: Rf = 49%, Violet solid, Yield: 38%, M.P. - 260.0^{0}C, FT-IR (ν in cm^{-1}): 3061, 1618, 1557, 1375, 1345, 1262, 1171. ^{1}H NMR (500 MHz, DMSO-d_6): δ = 8.72 (s, 1H), 7.93-7.91 (m, 1H), 7.81-7.79 (m, 1H), 7.6-7.53 (m, 2H), 6.76-6.74 (m, 1H), 6.3 (s, 2H), 6.27-6.25 (m, 1H), 6.21-6.19 (m, 1H), 5.2 (s, 2H), 3.8 (s, 3H), 3.39-3.32 (m, 8H), 1.22-1.15 (m, 12H) ppm. ^{13}C NMR (125 MHz, DMSO-d_6): 165.6, 163.5, 160.8, 152.7, 147.2, 143, 135.5, 131.6, 129.5, 126.2, 125.6, 125.1, 123.3, 121.8, 115, 113, 111.6, 105.8, 103.5, 94.5, 62.4, 51.8, 45, 36, 31.5, 29.5, 12.7, 12.4 ppm. HRMS: *m/z* calculated for $C_{35}H_{40}N_7OS_2$ [M - I] 638.2736, found 638.2725.

RF10: Rf = 54%, Violet solid, Yield: 50%, M.P. - 202.0^{0}C, FT-IR (ν in cm^{-1}): 3070, 1615, 1560, 1410, 1355, 1199. ^{1}H NMR (500 MHz, DMSO-d_6): δ = 8.44 (d, J = 8.25 Hz, 1H), 8.27 (d, J = 8.25 Hz, 1H), 8.20 (d, J = 8.25 Hz, 1H), 8.04-7.98 (m, 2H), 7.90-7.78 (m, 2H), 7.78-7.76 (m, 1H), 7.61-7.57 (m, 1H), 7.48-7.45 (m, 1H), 6.46-6.44 (m, 1H), 6.14-6.13 (m, 1H), 4.19-4.16 (m, 2H), 4.0 (s, 3H),3.51-3.47 (q, J = 6.85 Hz, 3H), 1.47 (t, J = 6.85 Hz, 3H), 1.15 (t, J = 6.85 Hz, 6H) ppm. ^{13}C NMR (125 MHz, DMSO-d_6): 173.2, 160.5, 154.6, 152.8, 150.3, 145.9, 144.7, 142.4, 140.2, 127.1, 126.0, 125.9, 124.9, 123.9, 119.9, 115.4, 112.1, 110, 94.7, 61.8, 46.7, 44.7, 35.2, 12.7 ppm. HRMS: *m/z* calculated for $C_{22}H_{27}N_2OS$ [M - I] 367.1844, found 367.1840.

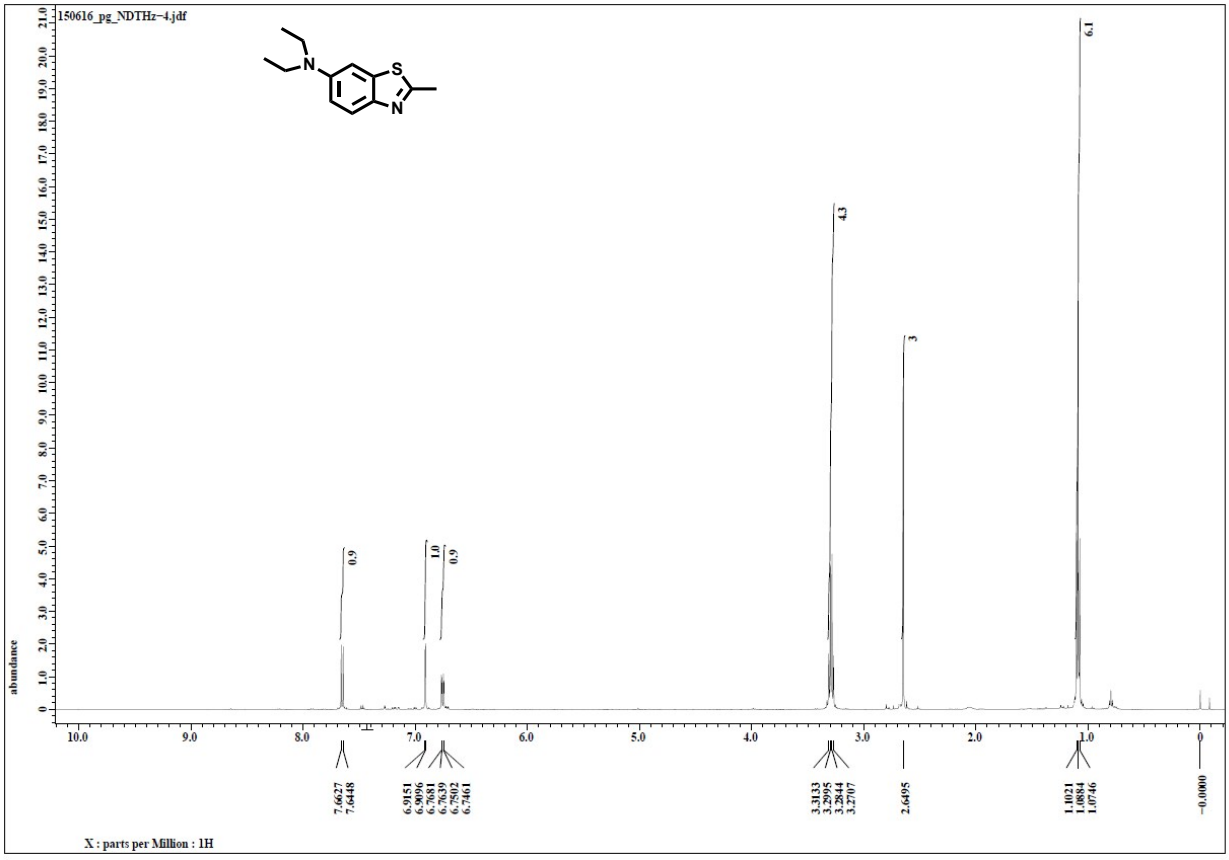

Fig. S11: ^{1}H-NMR

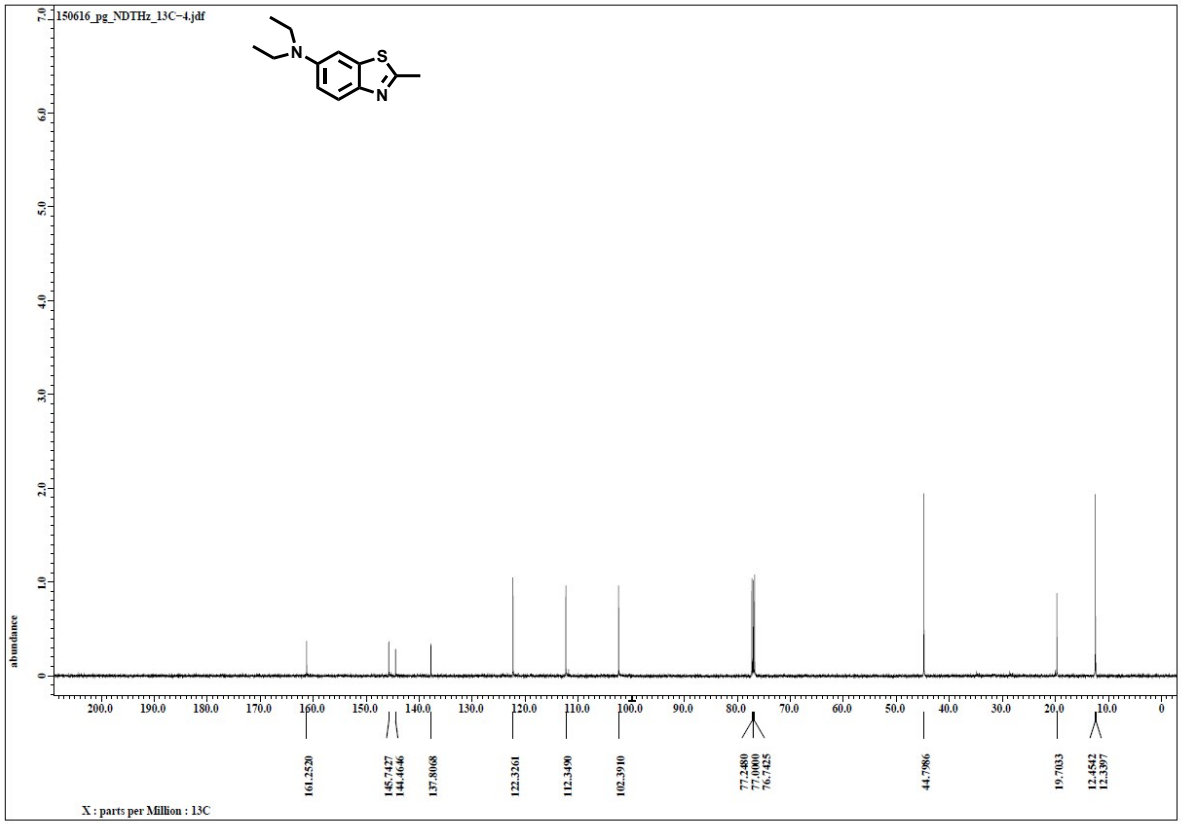

Fig. S12: ^{13}CNMR

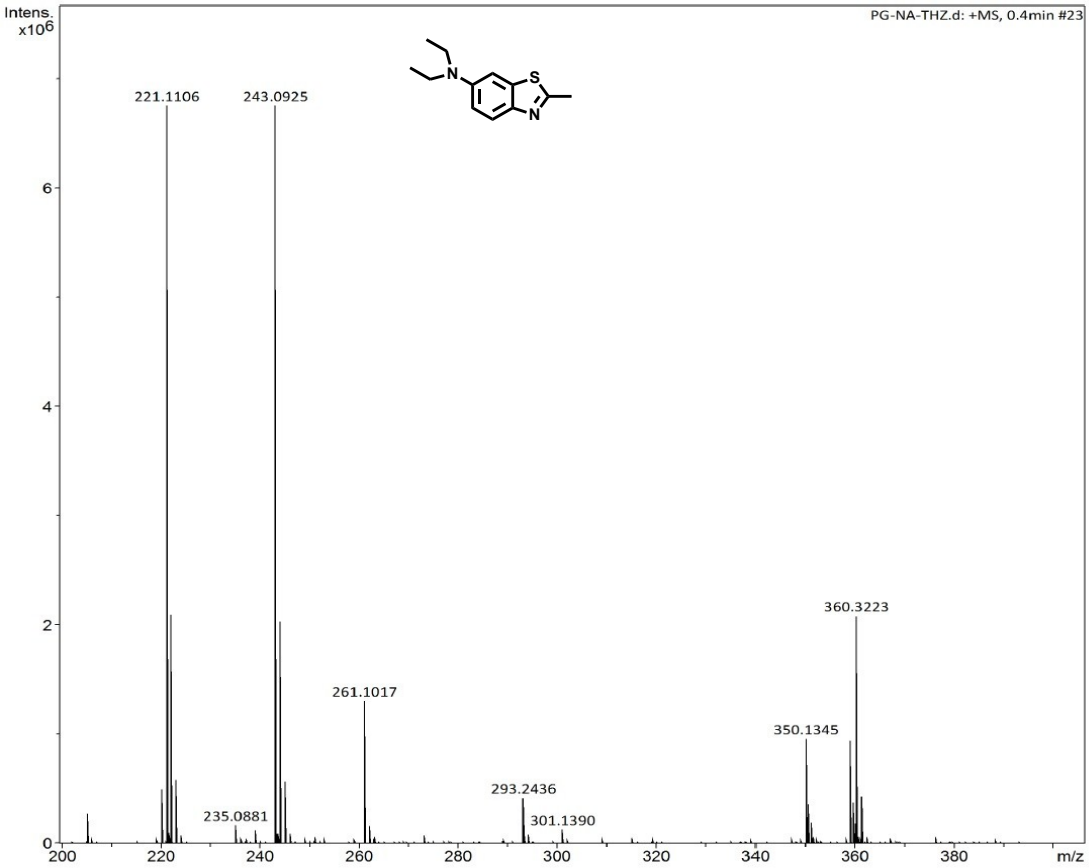

Fig. S13: HRMS

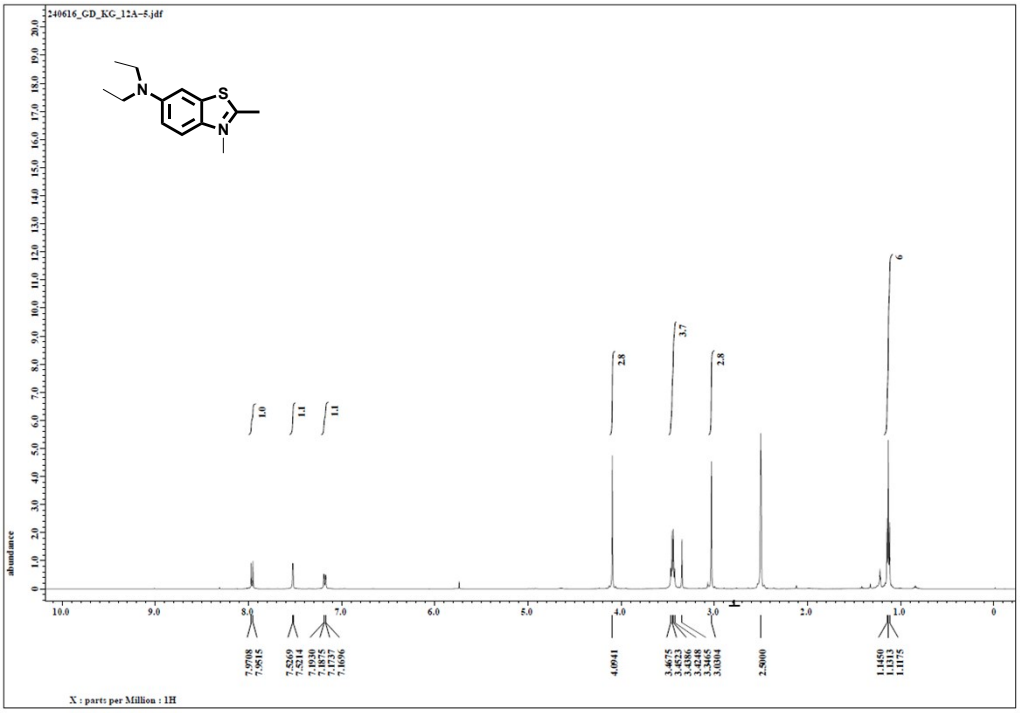

Fig. S14: ^{1}H-NMR

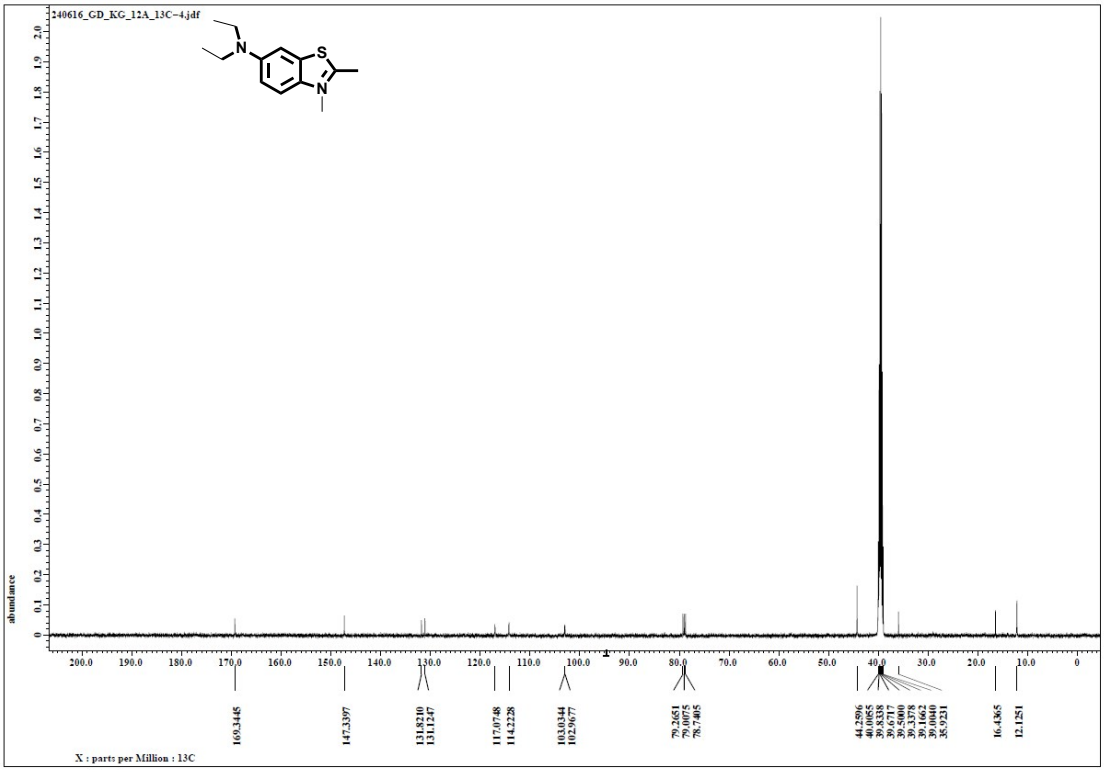

Fig. S15: ^{13}CNMR

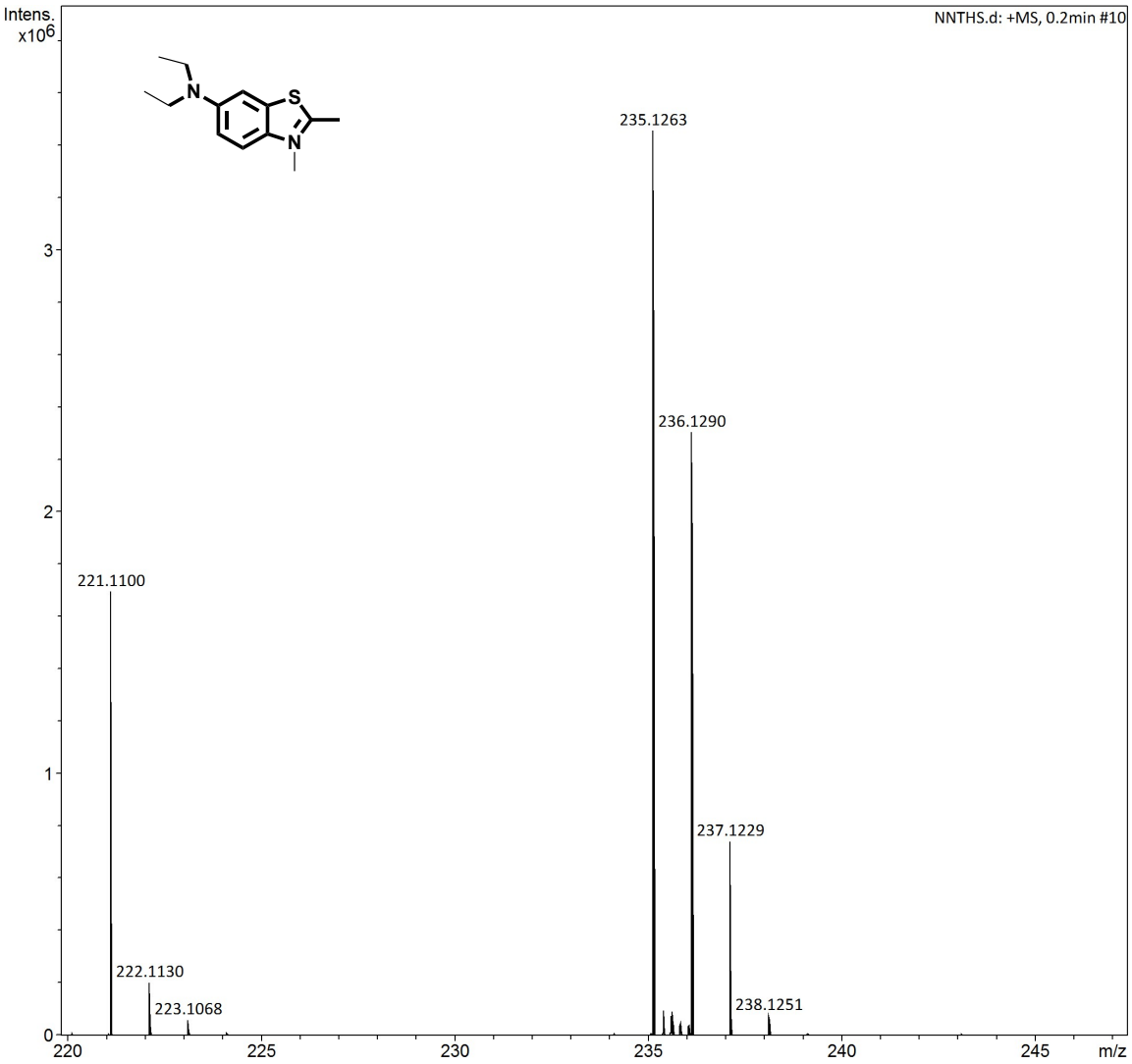
Intens.
x10^6
NNTHS.d: +MS, 0.2min #10
235.1263
236.1290
221.1100
237.1229
222.1130
223.1068
238.1251
0
1
2
3
220
225
230
235
240
245
m/z

Fig. S16: HRMS

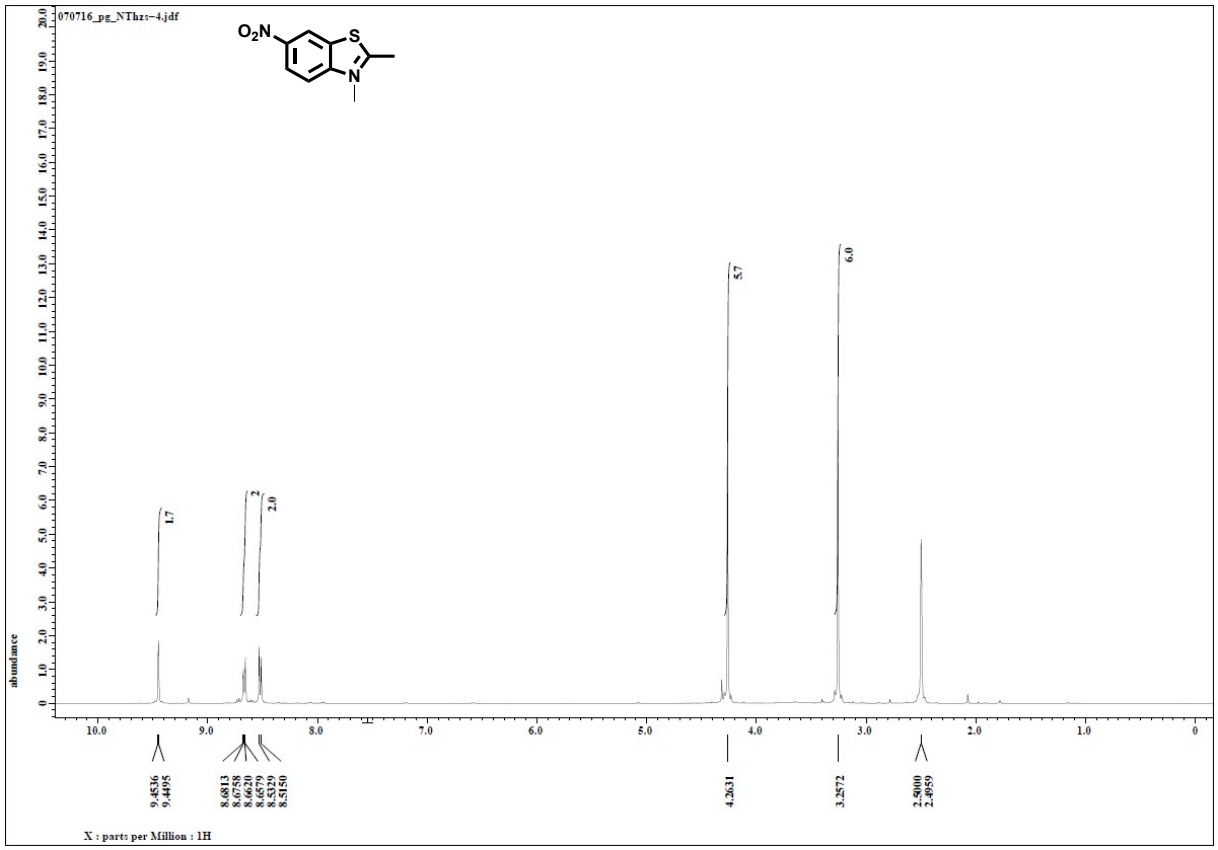

Fig. S17: ^{1}H-NMR

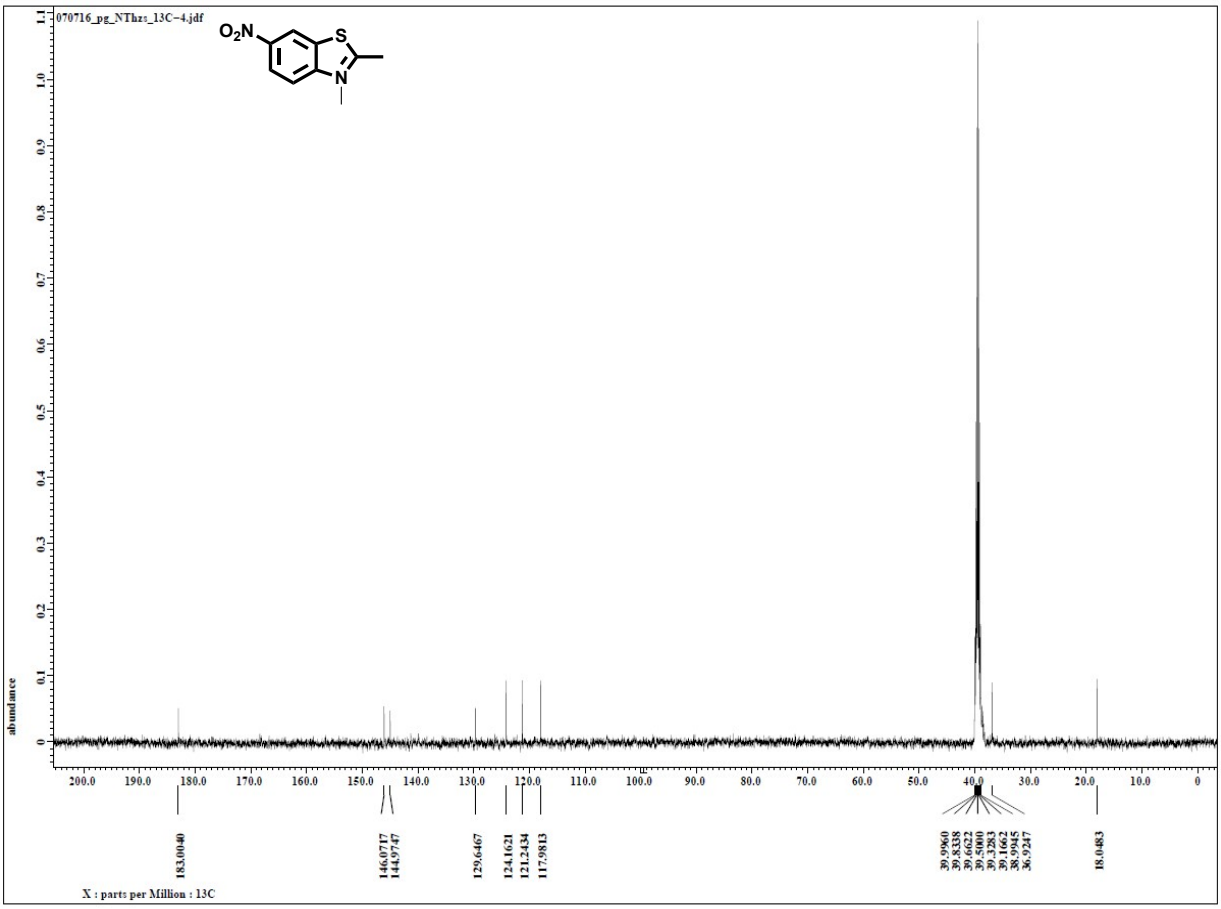

Fig. S18: ^{13}CNMR

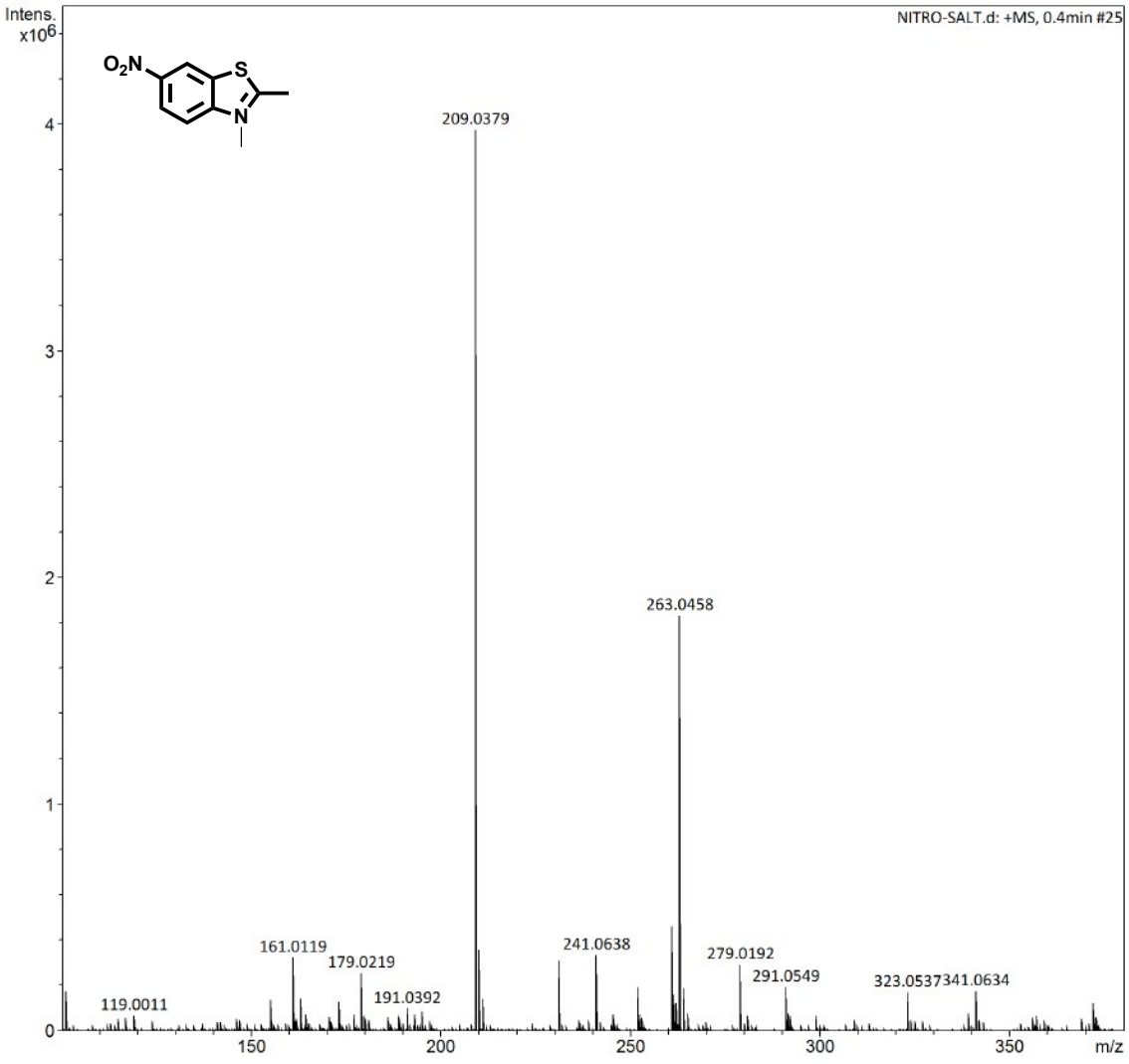
Intens.
x10^6
NITRO-SALT.d: +MS, 0.4min #25
O2N
S
N
209.0379
263.0458
161.0119
179.0219
191.0392
119.0011
241.0638
279.0192
291.0549
323.0537
341.0634
0
1
2
3
4
150
200
250
300
350
m/z

Fig. S19: HRMS

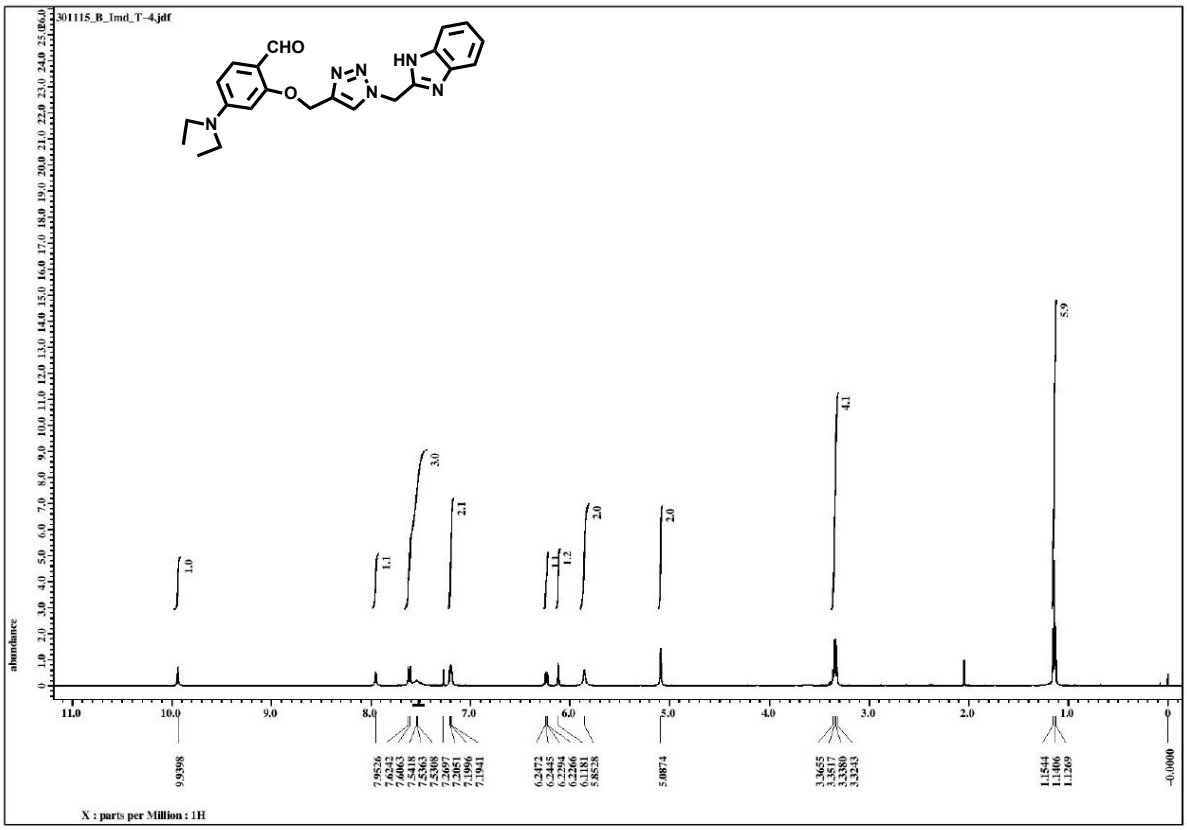

Fig. S20: ^{1}H-NMR

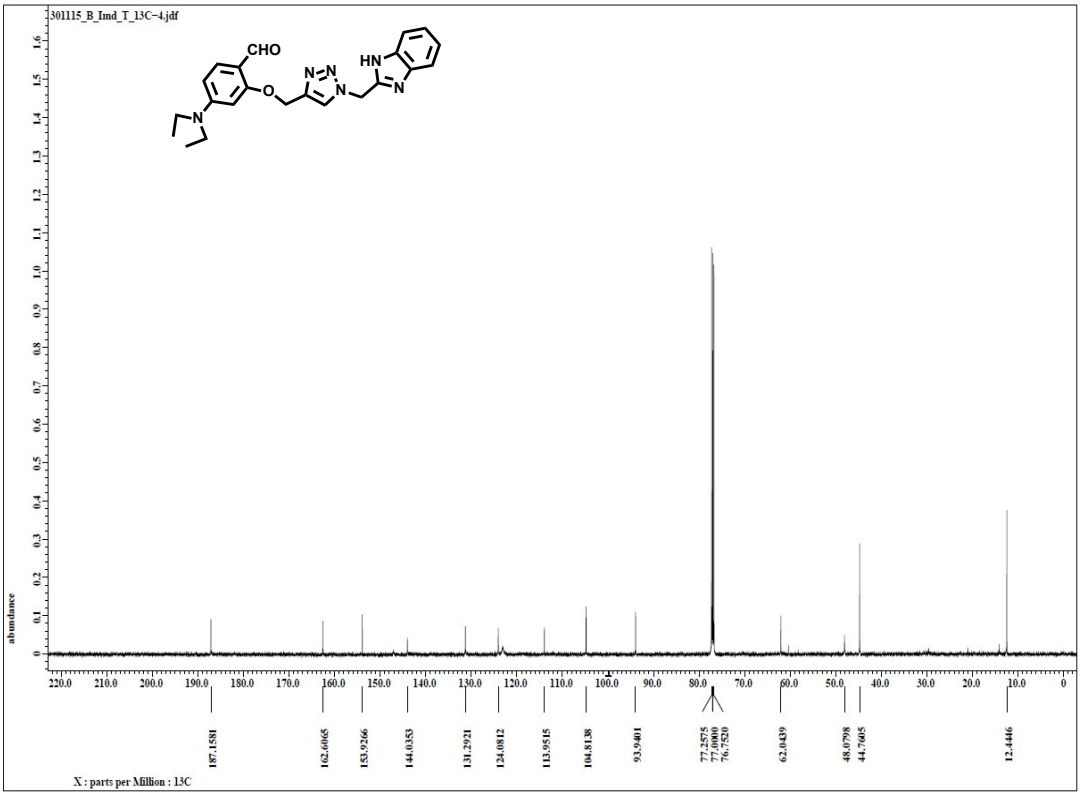

Fig. S21: ^{13}CNMR

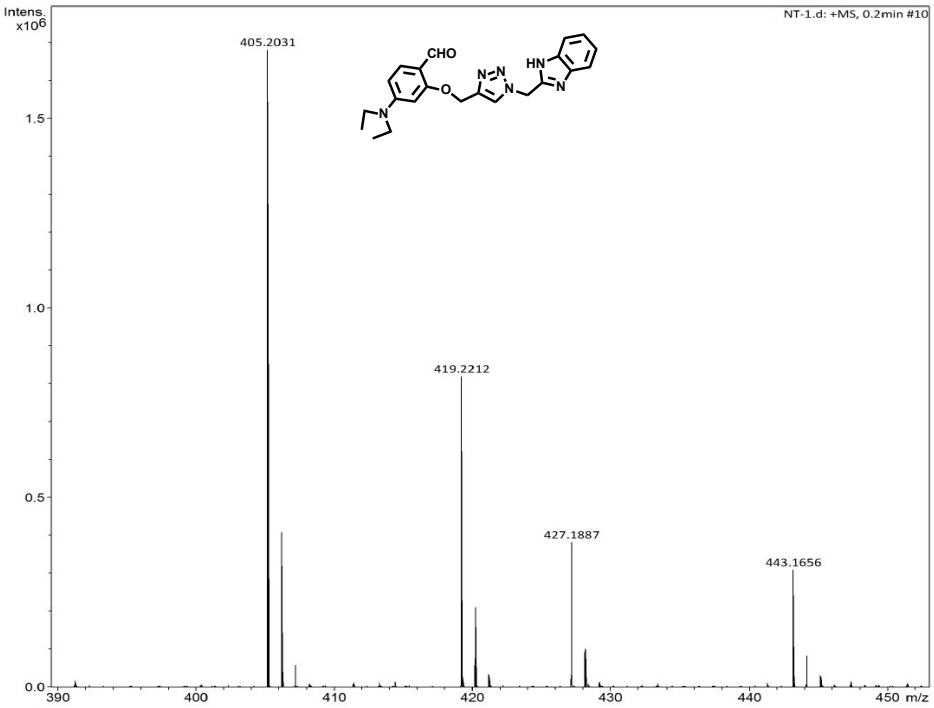

Fig. S22: HRMS

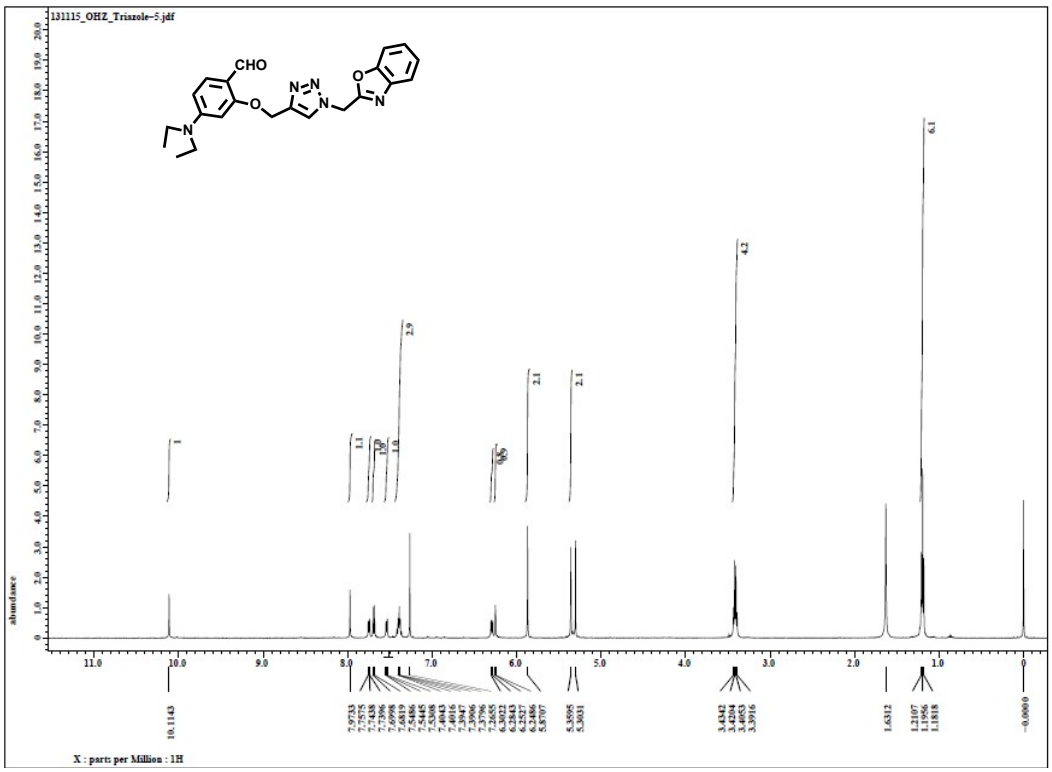

Fig. S23: ^{1}H-NMR

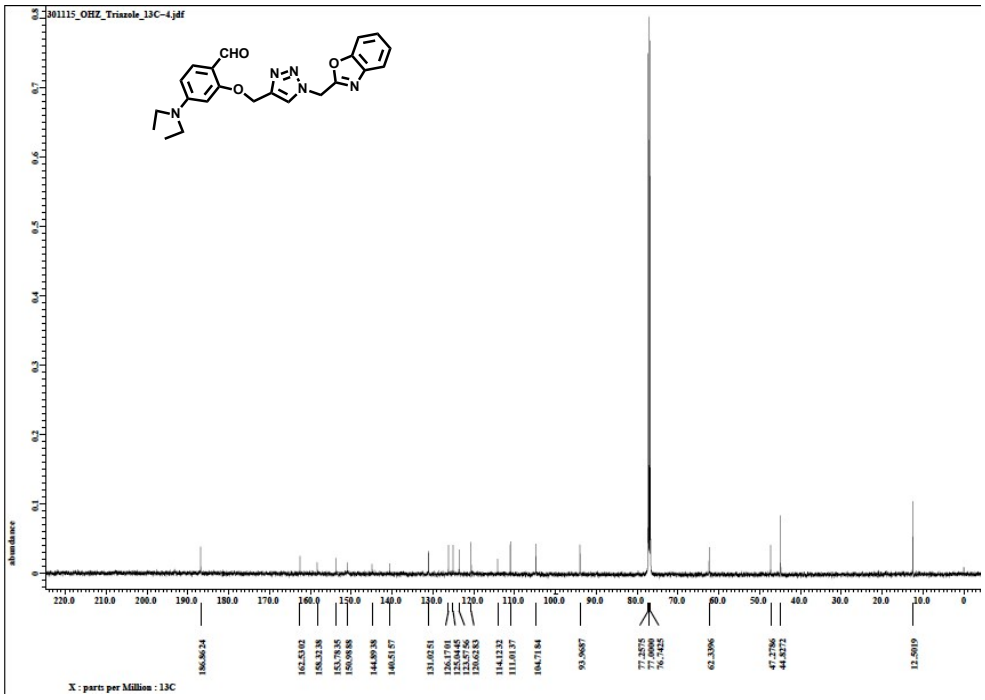

Fig. S24: ^{13}CNMR

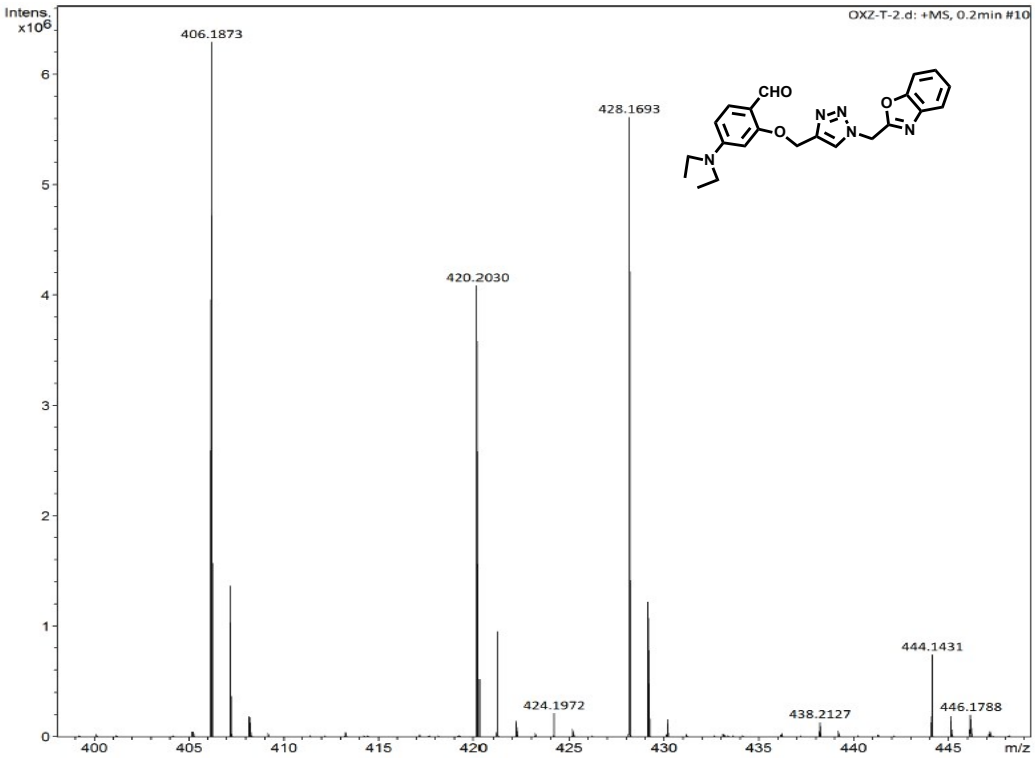
Intens.
x10^6
OXZ-T-2.d: +MS, 0.2min #10
406.1873
428.1693
420.2030
424.1972
438.2127
444.1431
446.1788
CHO
m/z

Fig. S25: HRMS

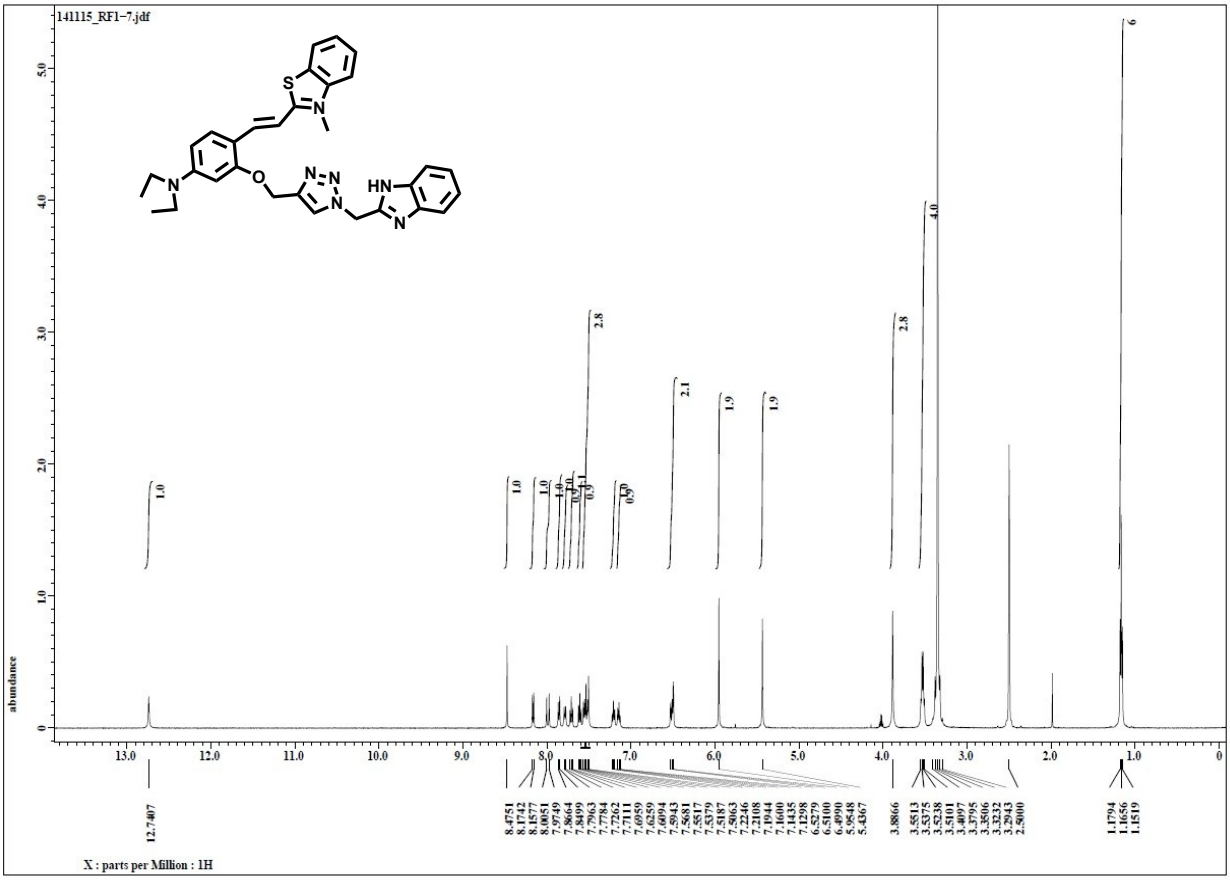

Fig. S26: ^{1}H-NMR

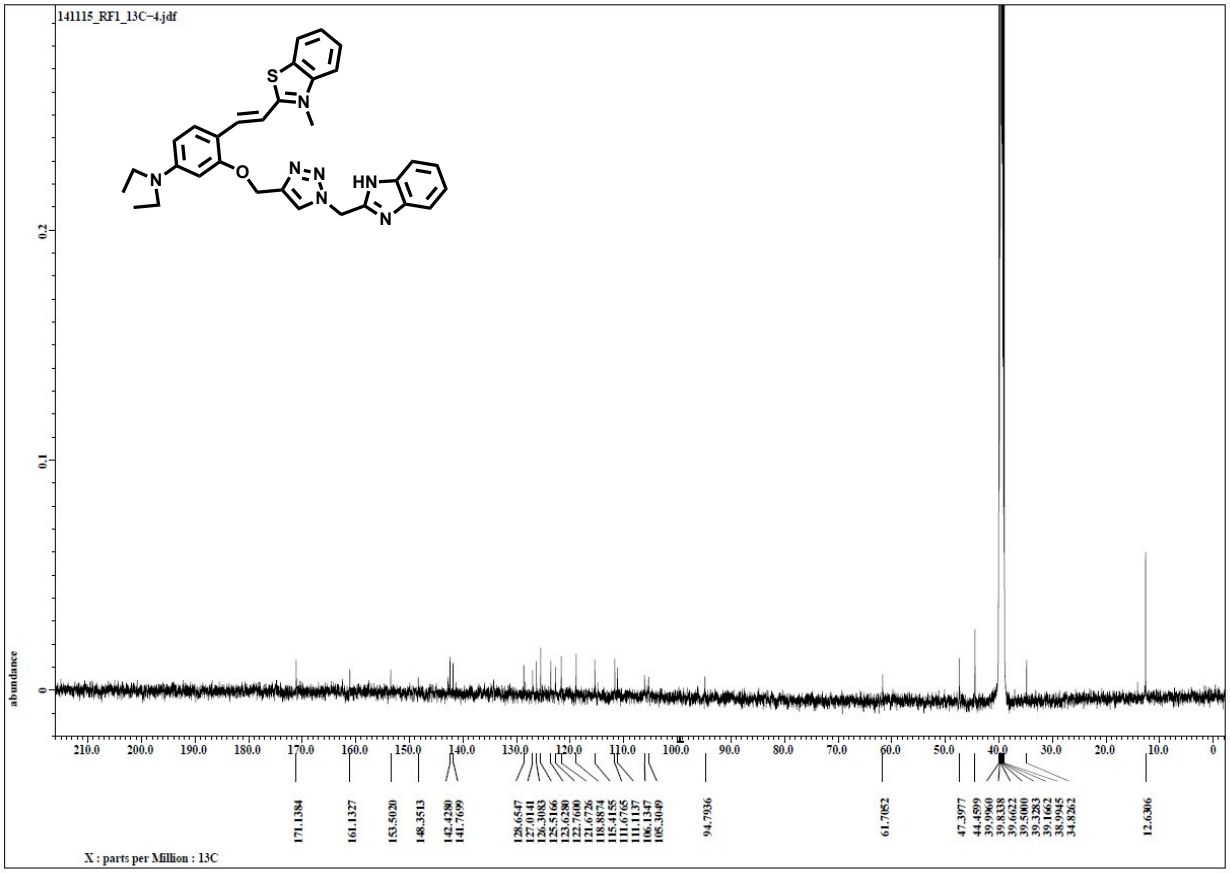

Fig. S27: ^{13}CNMR

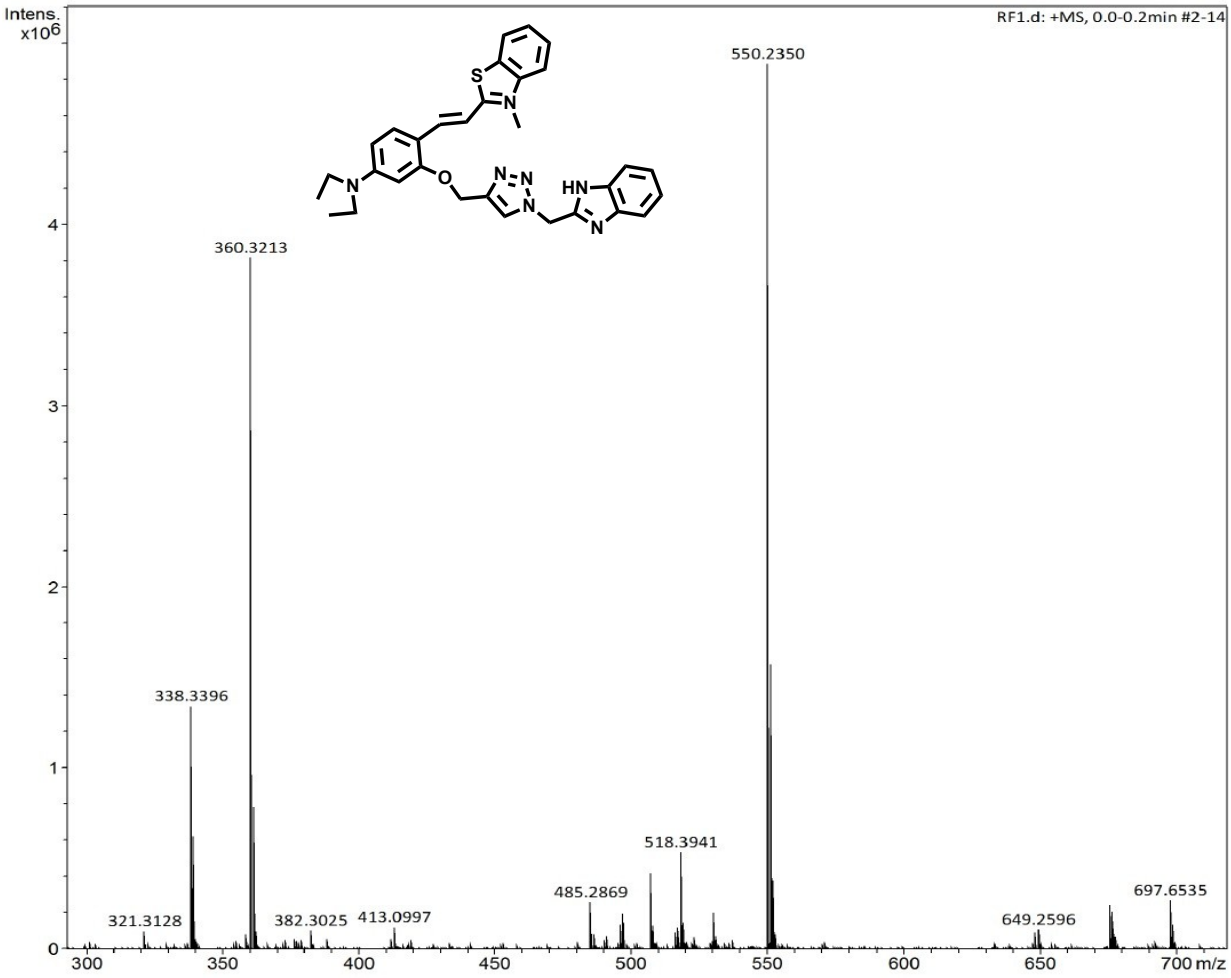
Intens.
x10^6
RF1.d: +MS, 0.0-0.2min #2-14
550.2350
360.3213
338.3396
518.3941
485.2869
697.6535
321.3128
382.3025
413.0997
649.2596
0
1
2
3
4
300
350
400
450
500
550
600
650
700 m/z

Fig. S28: HRMS

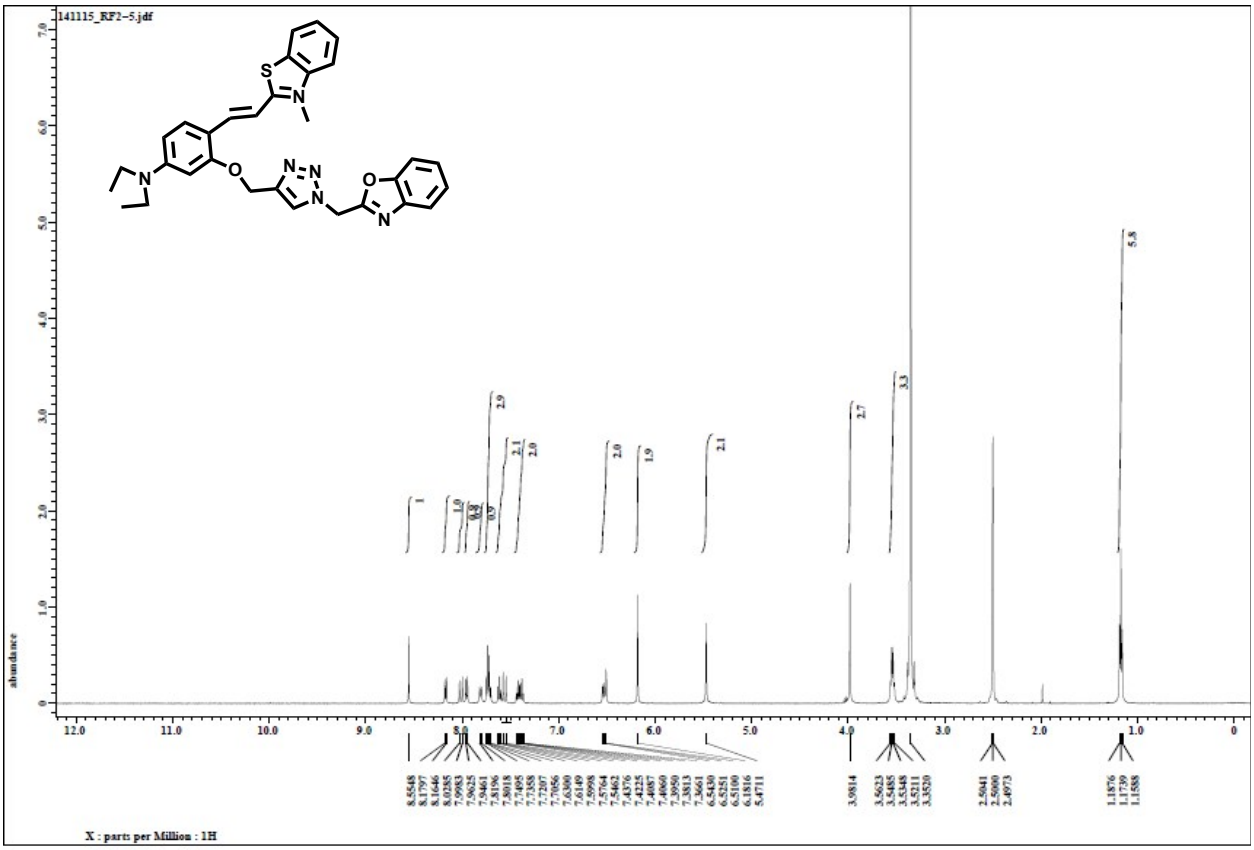

Fig. S29: ^{1}H-NMR

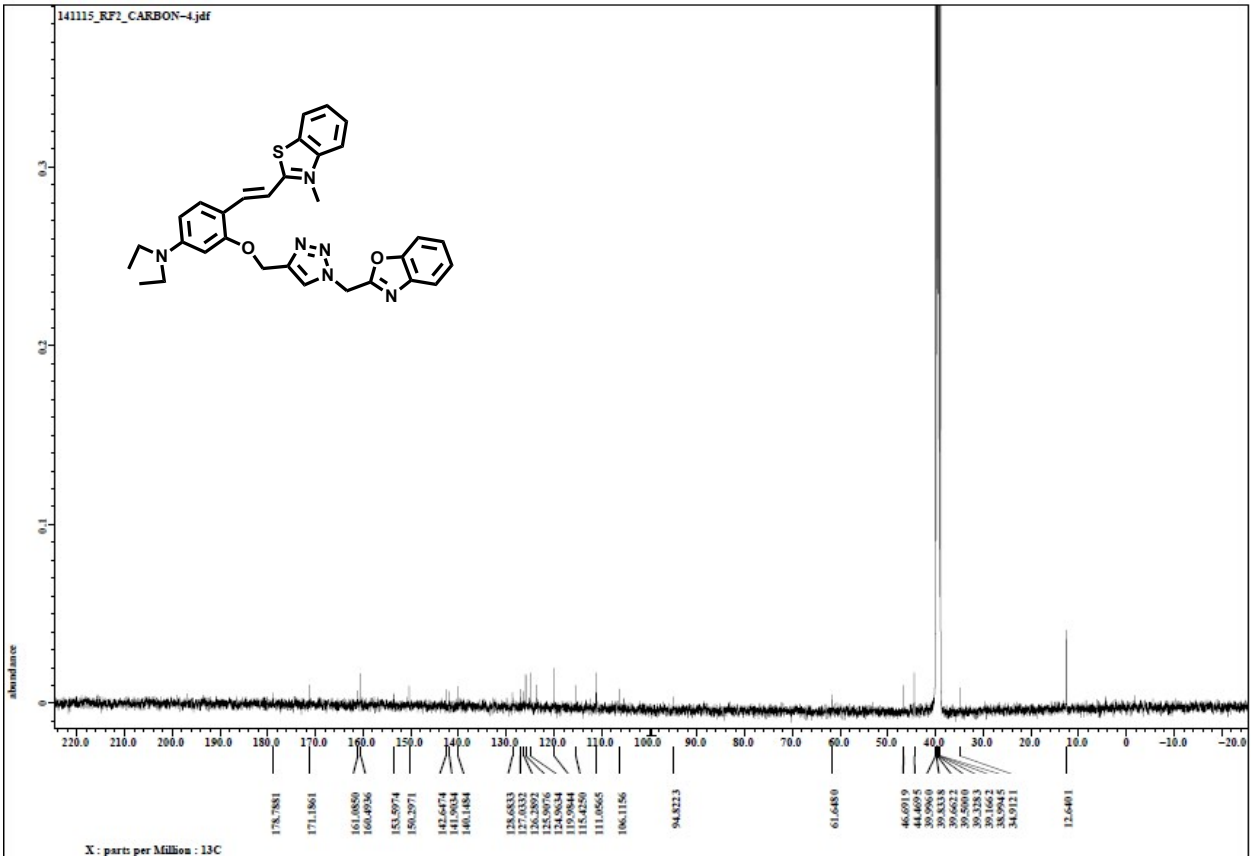

Fig. S30: ^{13}CNMR

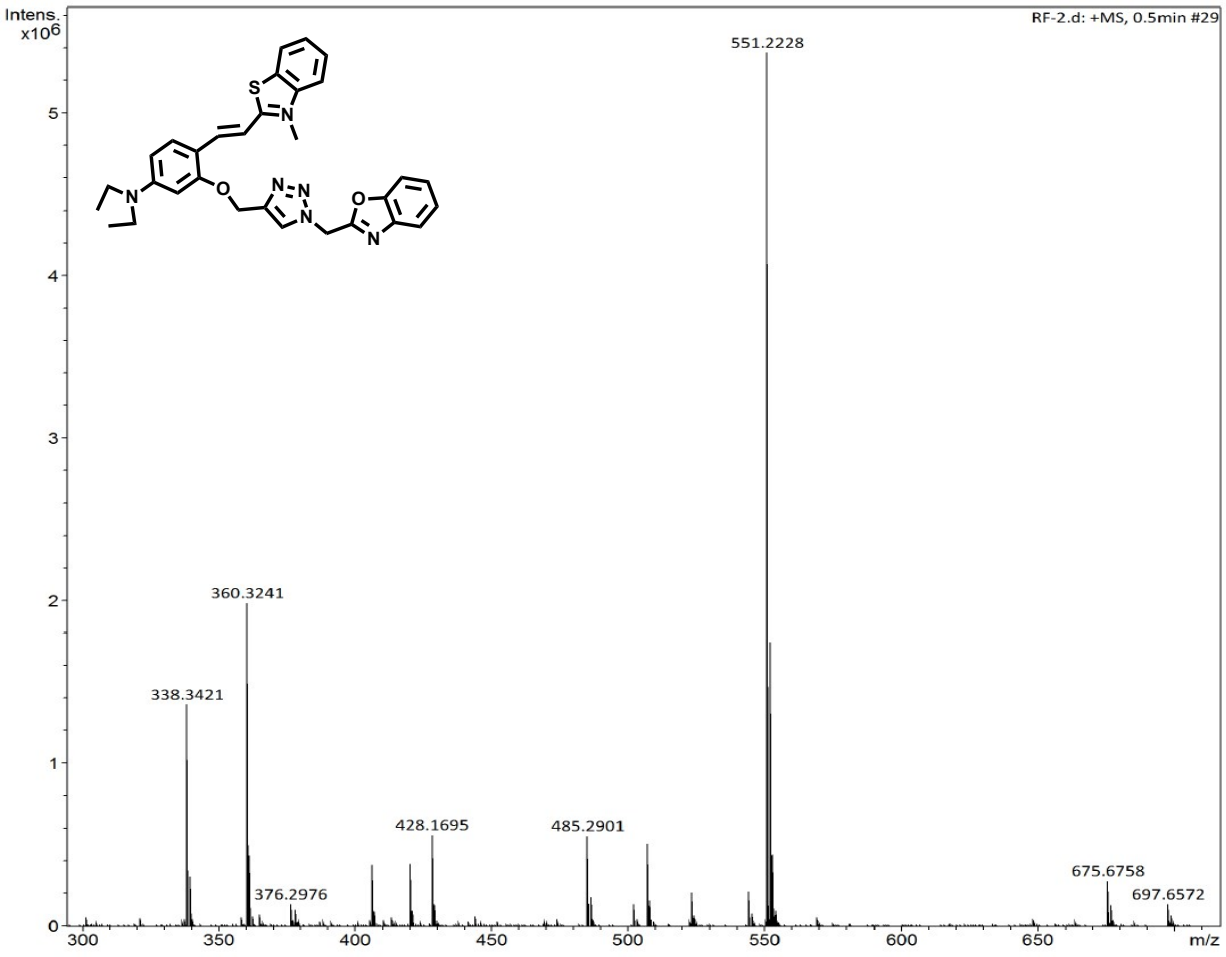
Intens.
x10^6
RF-2.d: +MS, 0.5min #29
551.2228
360.3241
338.3421
428.1695
485.2901
376.2976
675.6758
697.6572
m/z

Fig. S31: HRMS

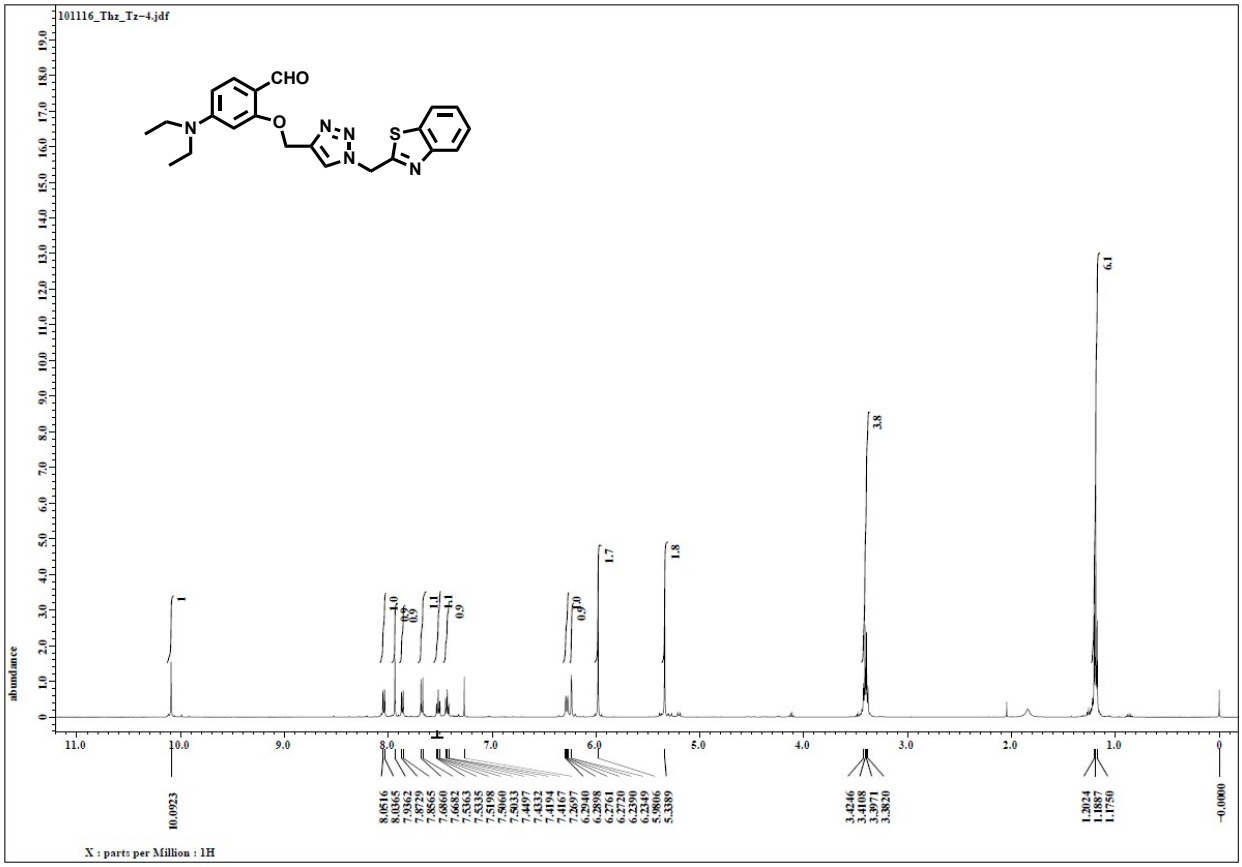

Fig. S32: ^{1}H-NMR

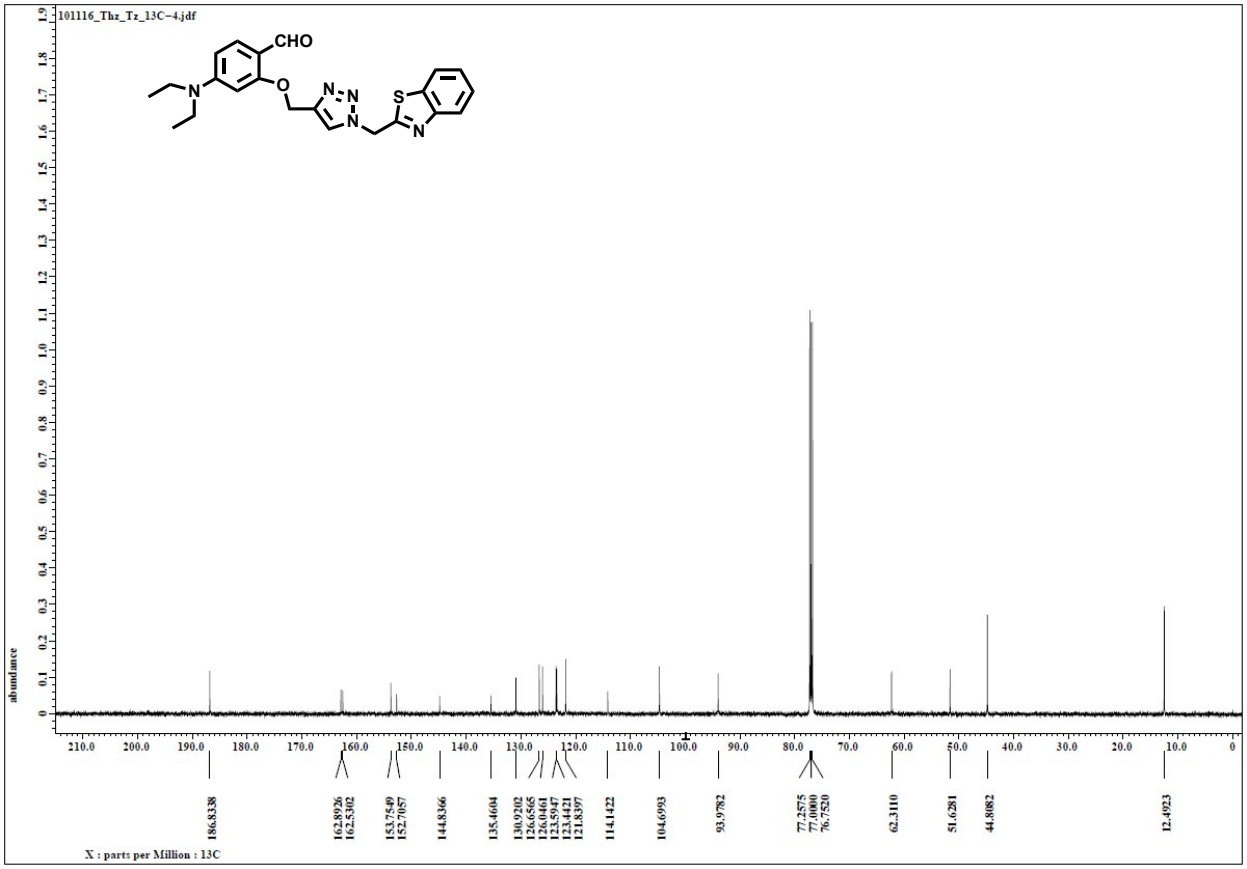

Fig. S33: ^{13}CNMR

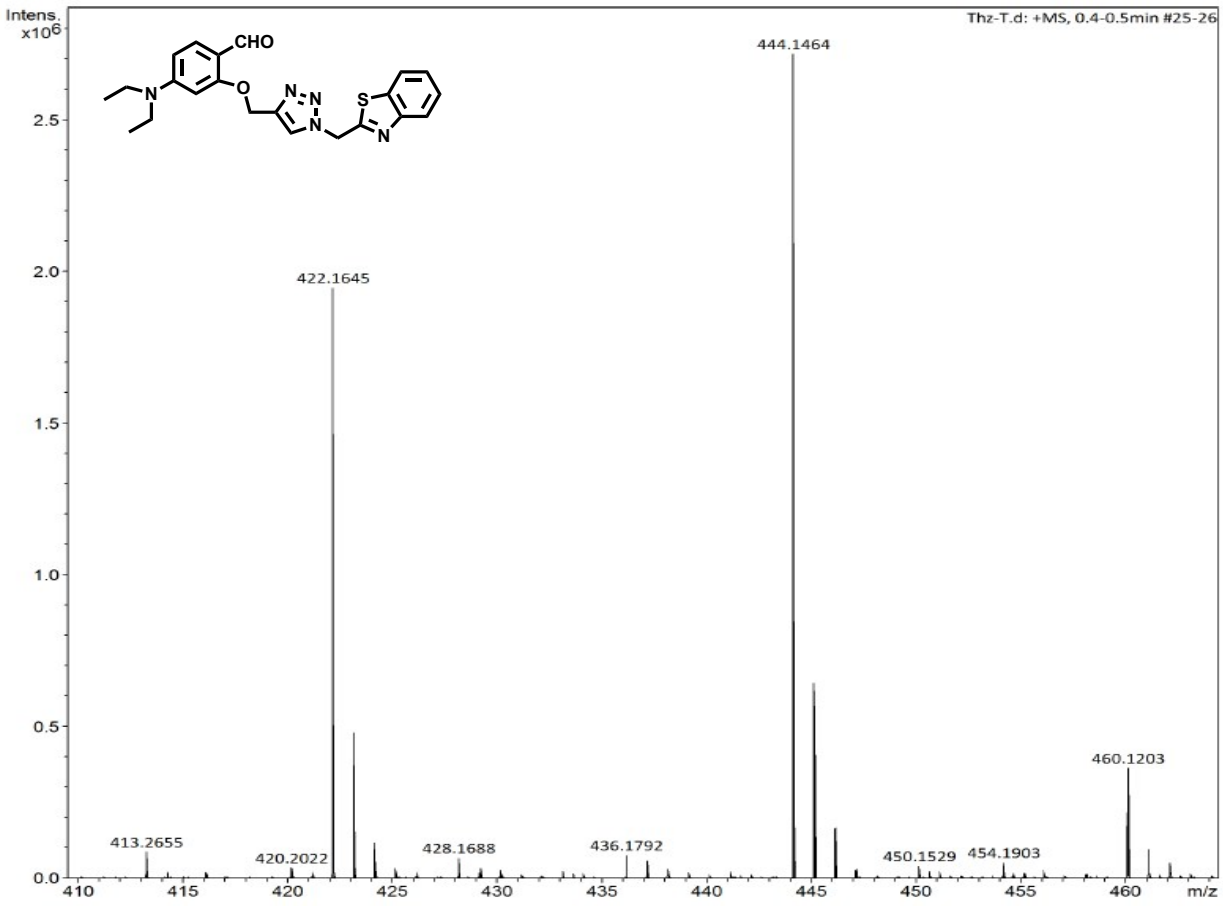
Intens.
x10^6
Thz-T.d: +MS, 0.4-0.5min #25-26
CHO
444.1464
422.1645
460.1203
413.2655
420.2022
428.1688
436.1792
450.1529
454.1903
m/z

Fig. S34: HRMS

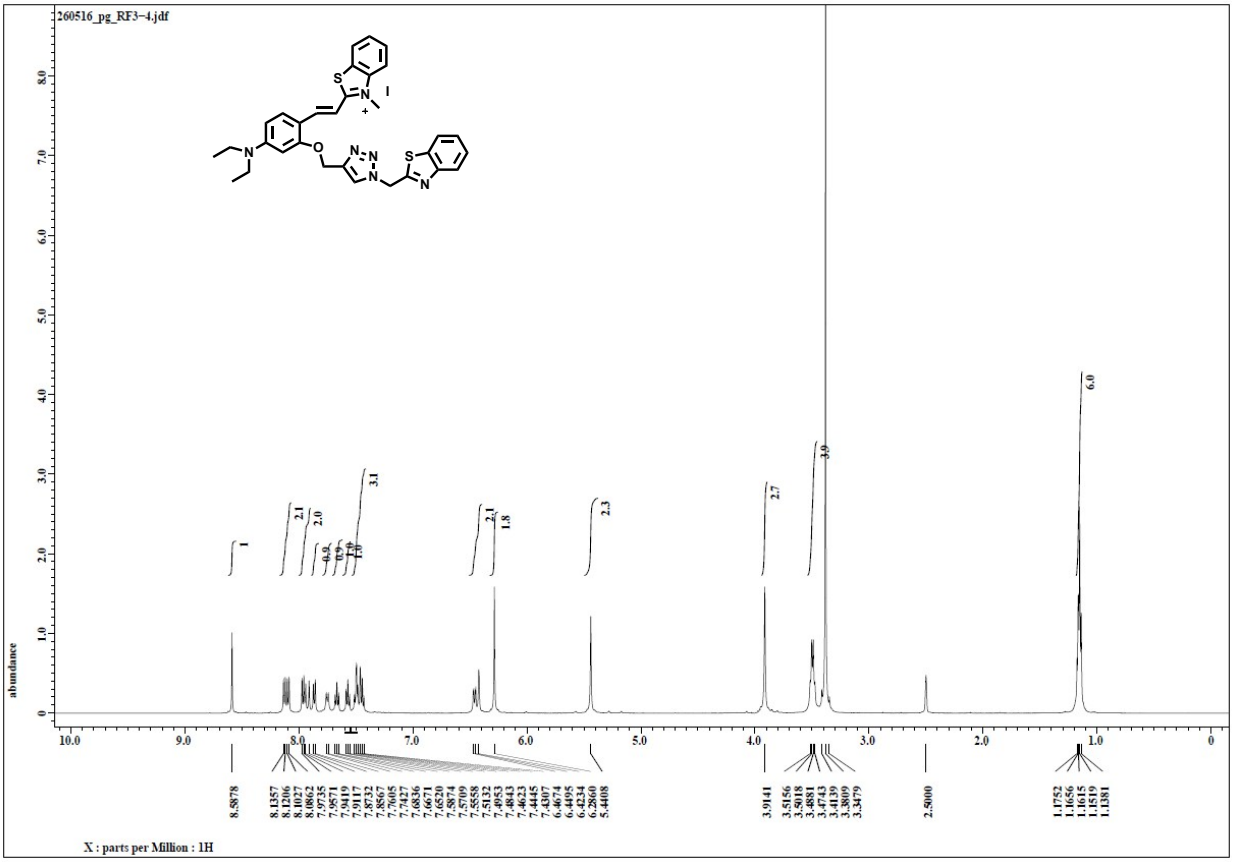

Fig. S35: ^{1}H-NMR

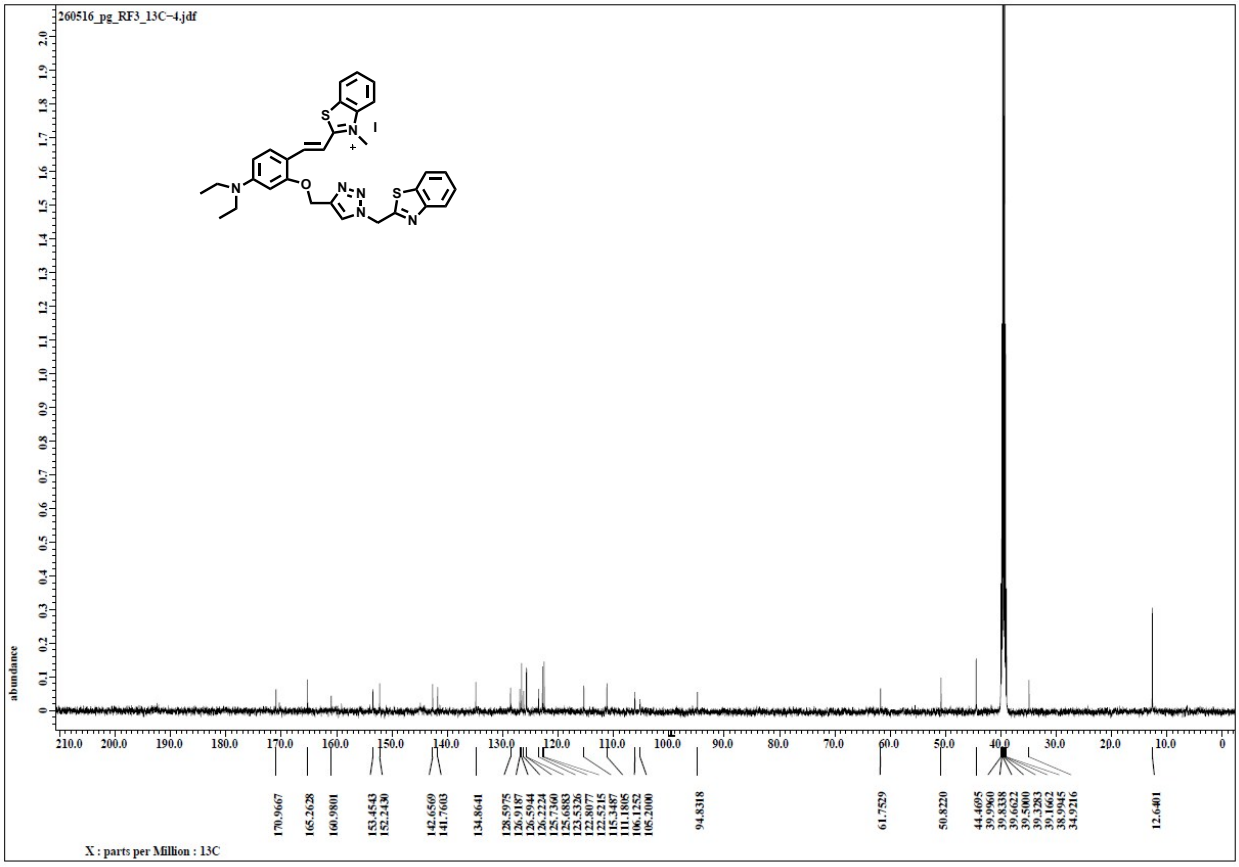

Fig. S36: ^{13}CNMR

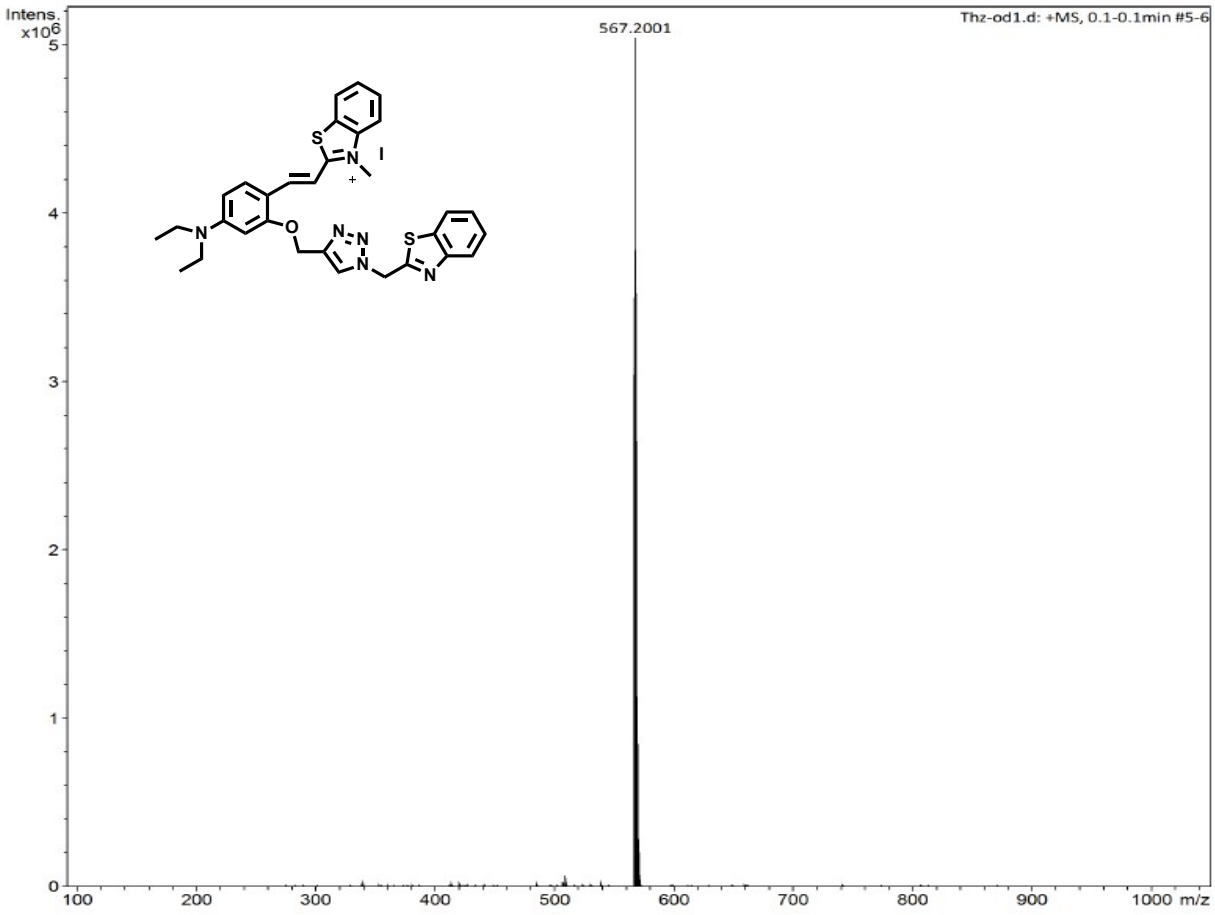
Intens.
x10^6
5
4
3
2
1
0
567.2001
Thz-od1.d: +MS, 0.1-0.1min #5-6
100
200
300
400
500
600
700
800
900
1000 m/z

Fig. S37: HRMS

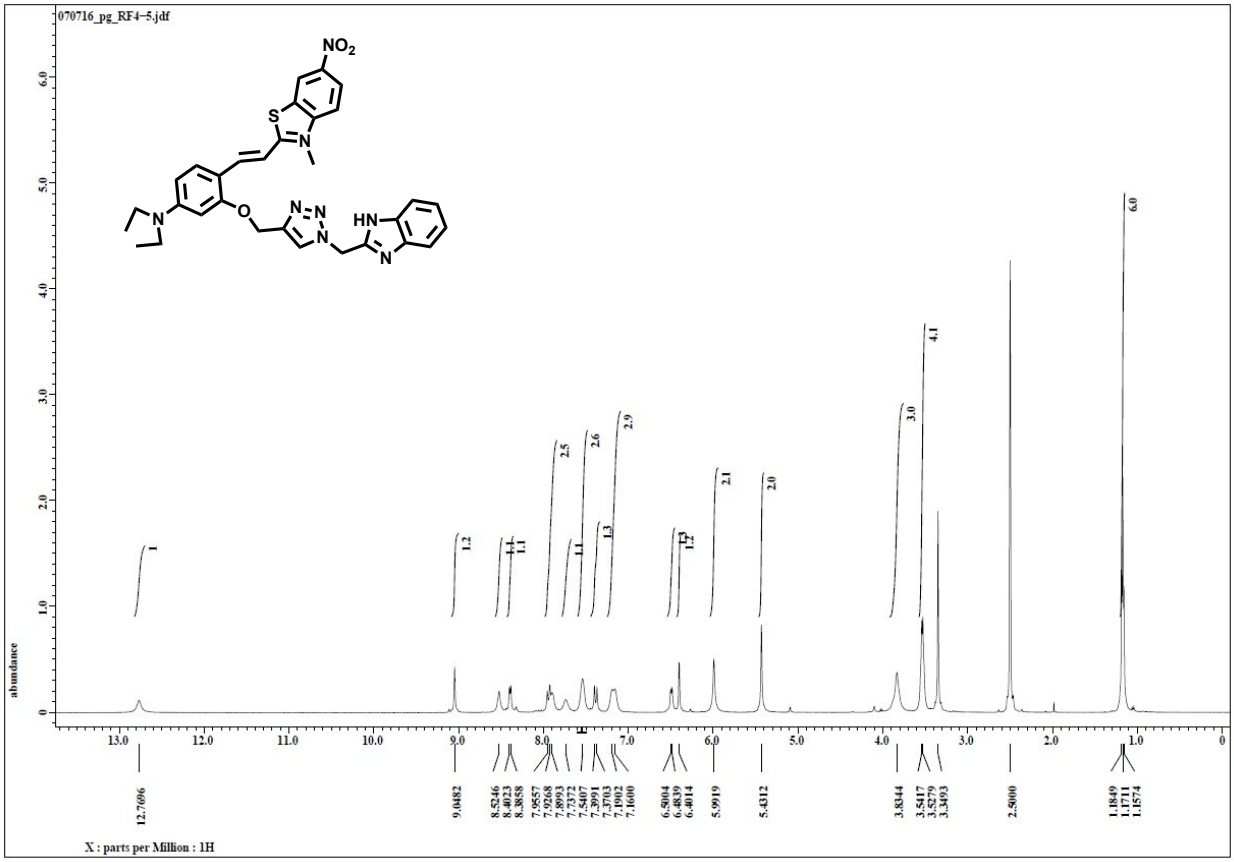

Fig. S38: ^{1}H-NMR

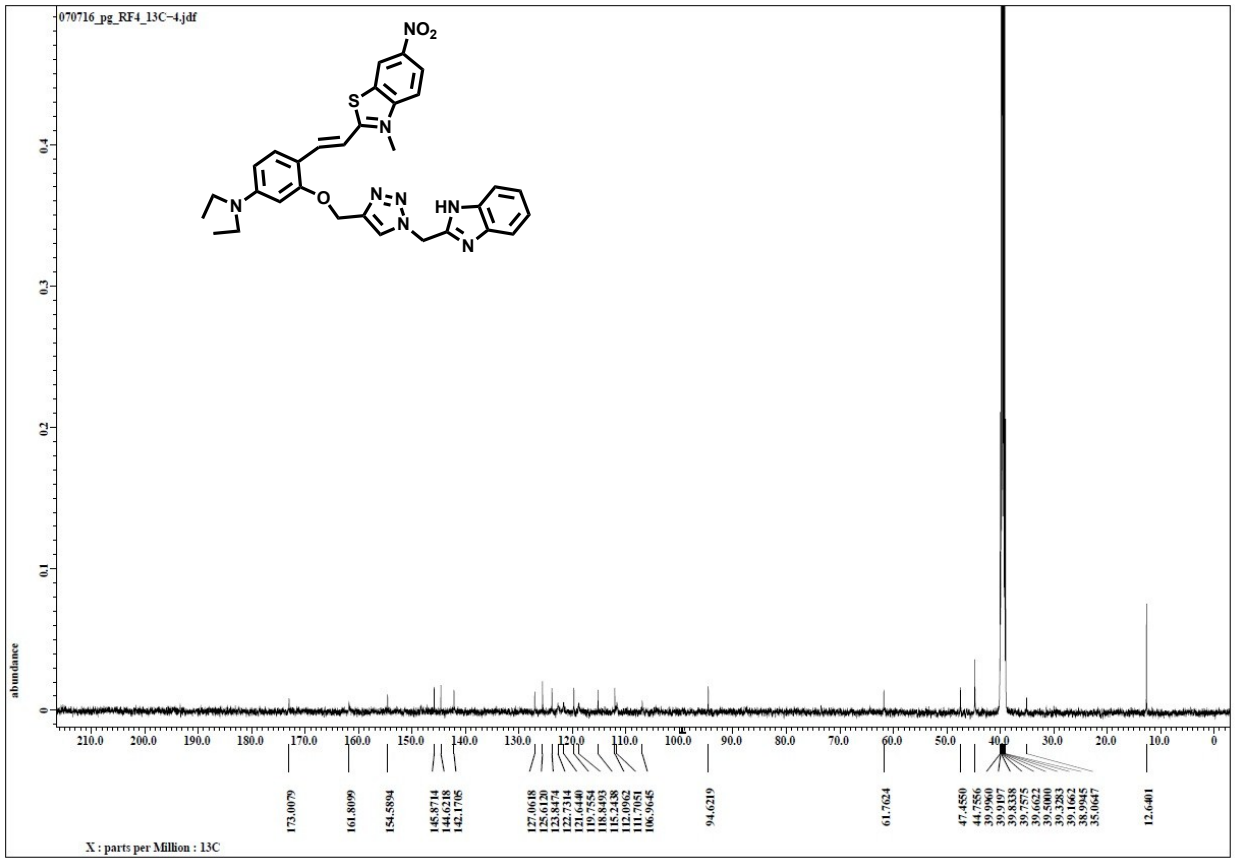

Fig. S39: ^{13}CNMR

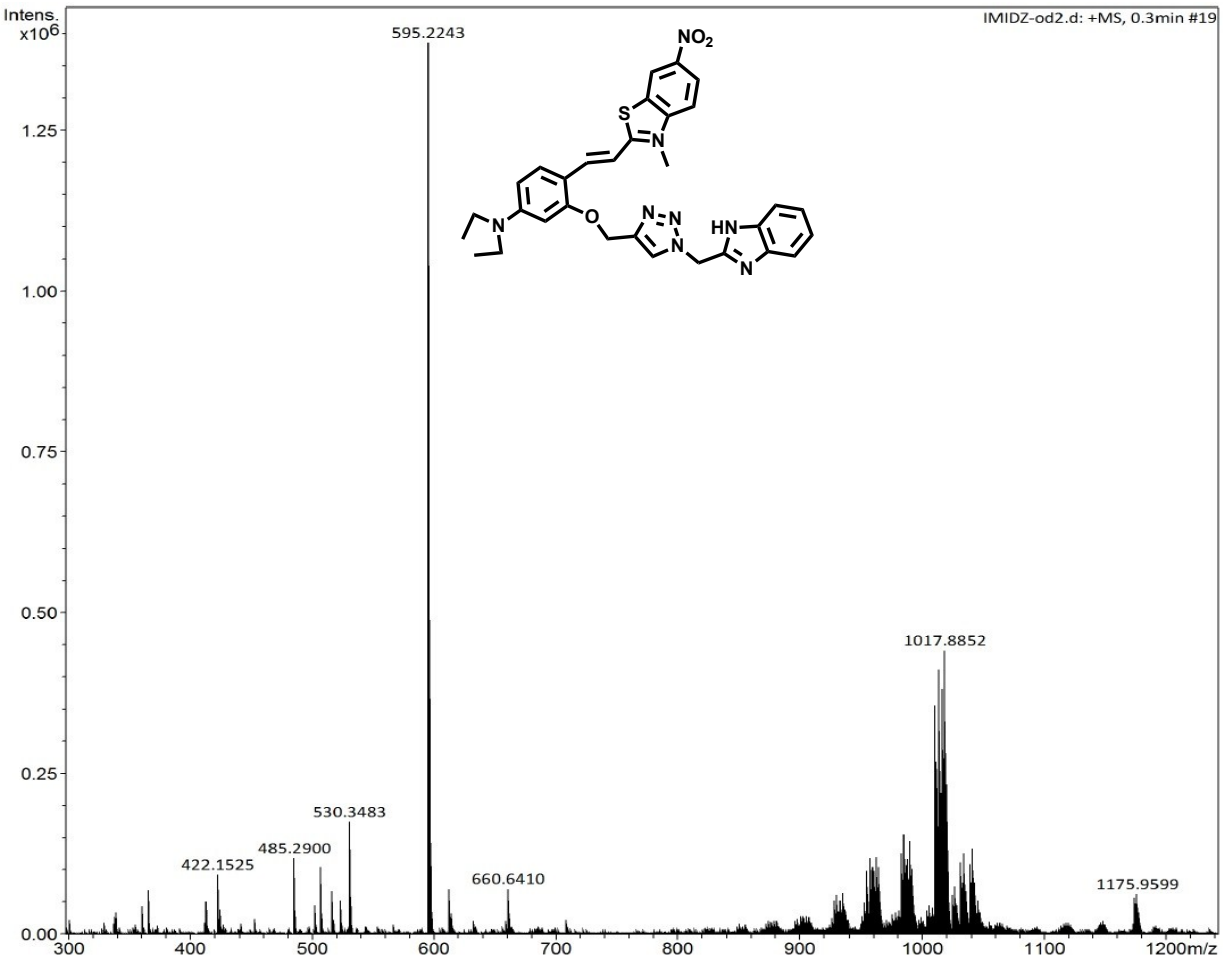
Intens.
x10^6
IMIDZ-od2.d: +MS, 0.3min #19
595.2243
1017.8852
530.3483
485.2900
422.1525
660.6410
1175.9599
1.25
1.00
0.75
0.50
0.25
0.00
300
400
500
600
700
800
900
1000
1100
1200m/z

Fig. S40: HRMS

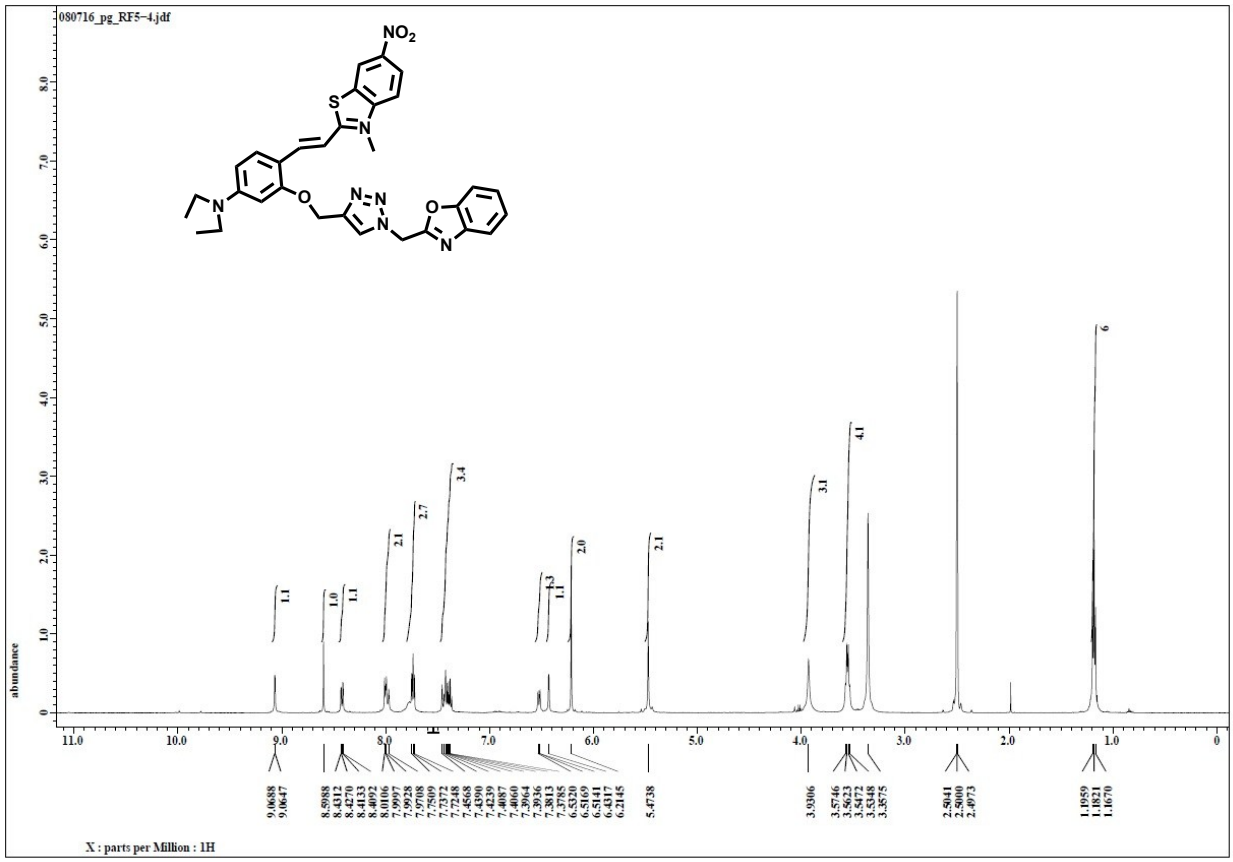

Fig. S41: ^{1}H-NMR

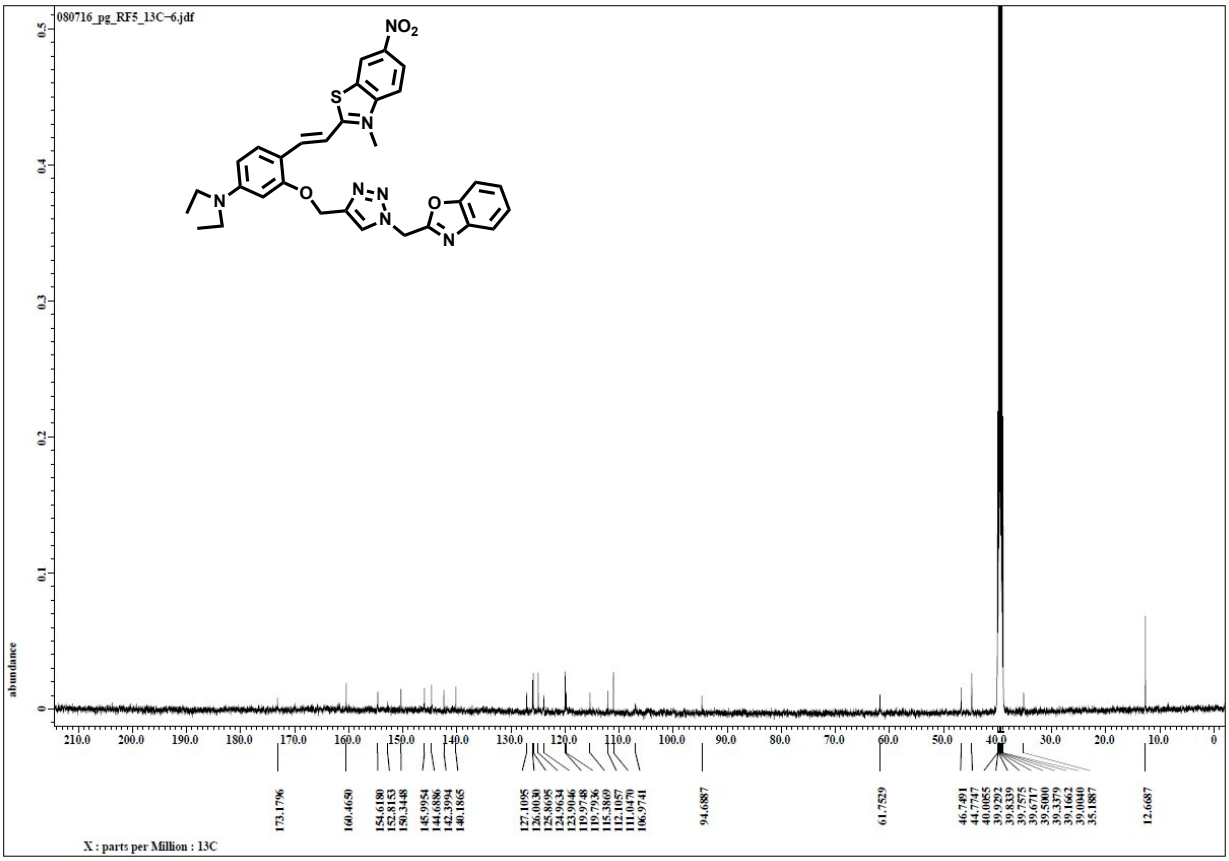

Fig. S42: ^{13}CNMR

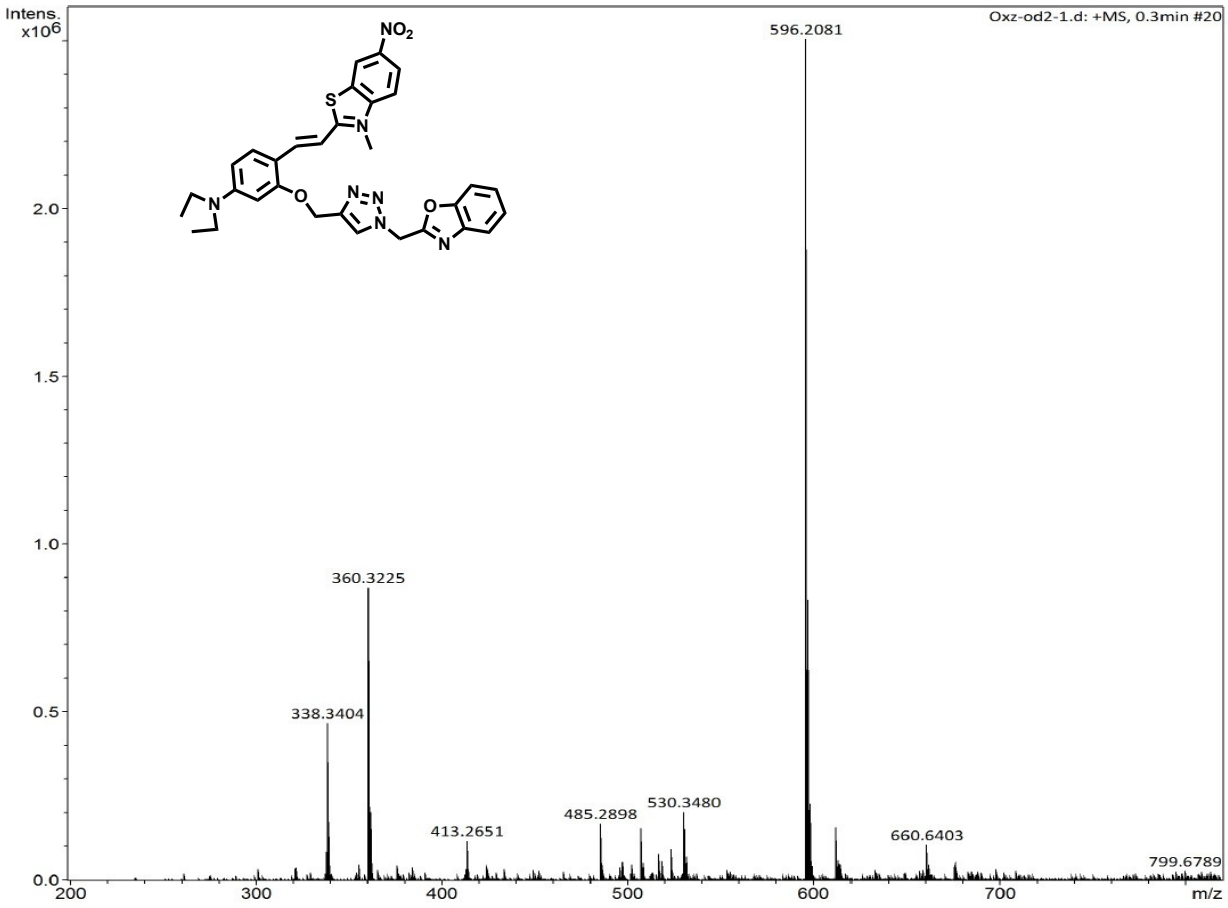
Intens.
x10^6
Oxz-od2-1.d: +MS, 0.3min #20
596.2081
360.3225
338.3404
413.2651
485.2898
530.3480
660.6403
799.6789
m/z

Fig. S43: HRMS

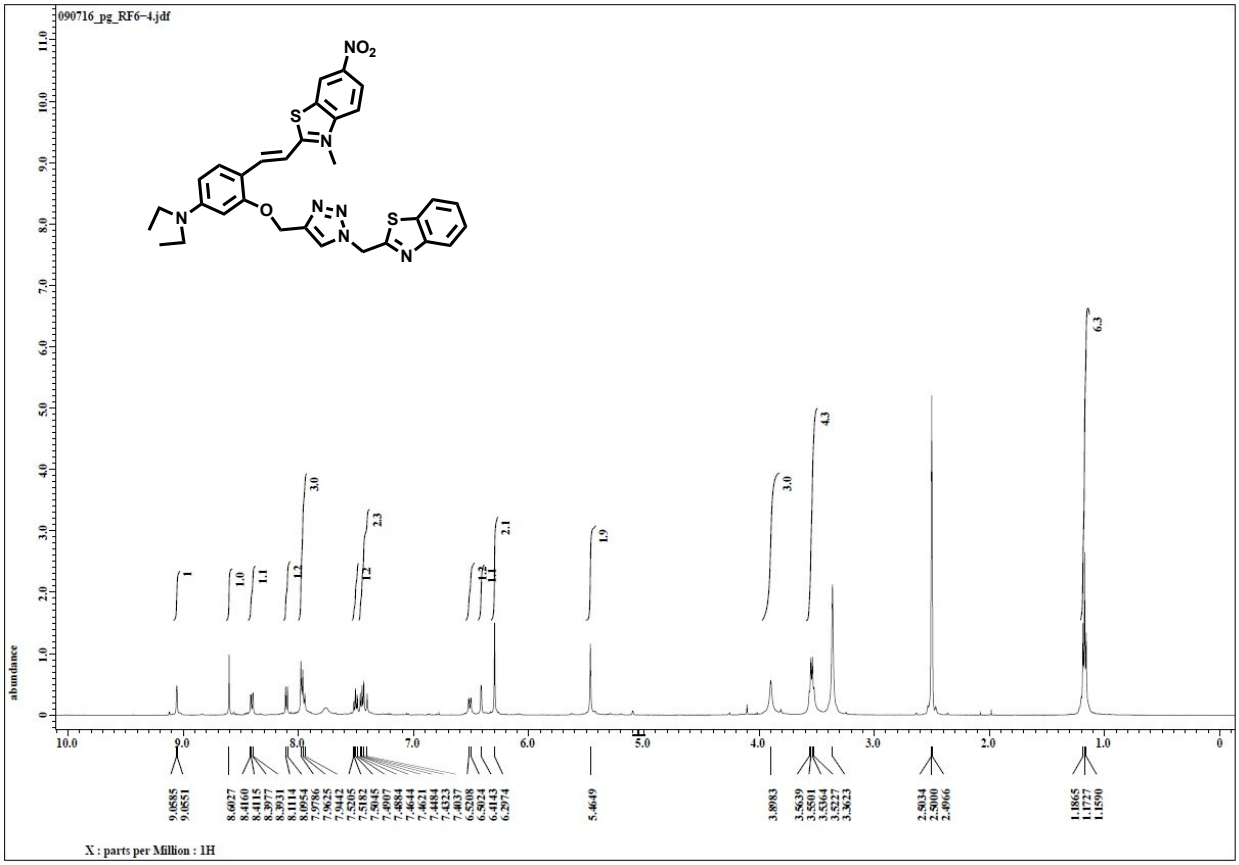

Fig. S44: ^{1}H-NMR

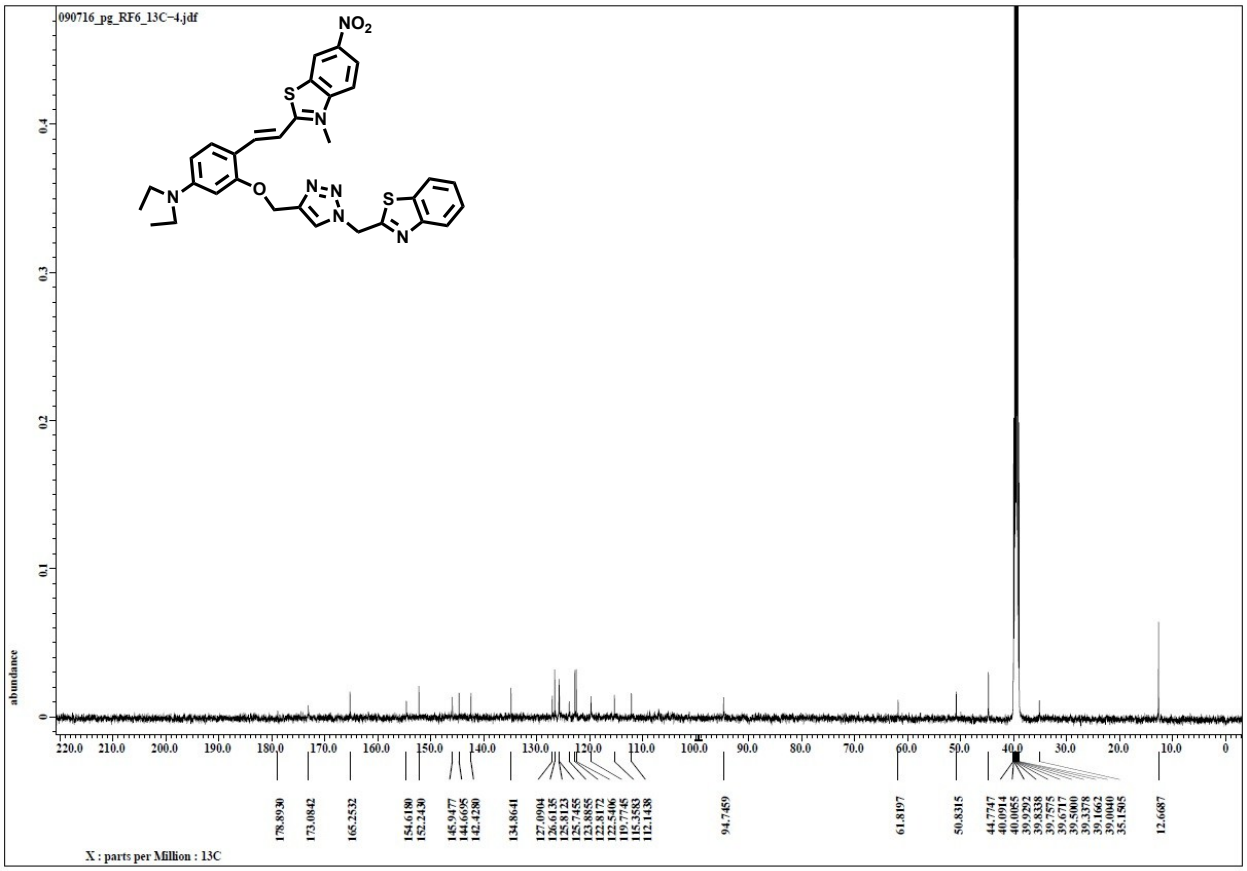

Fig. S45: ^{13}CNMR

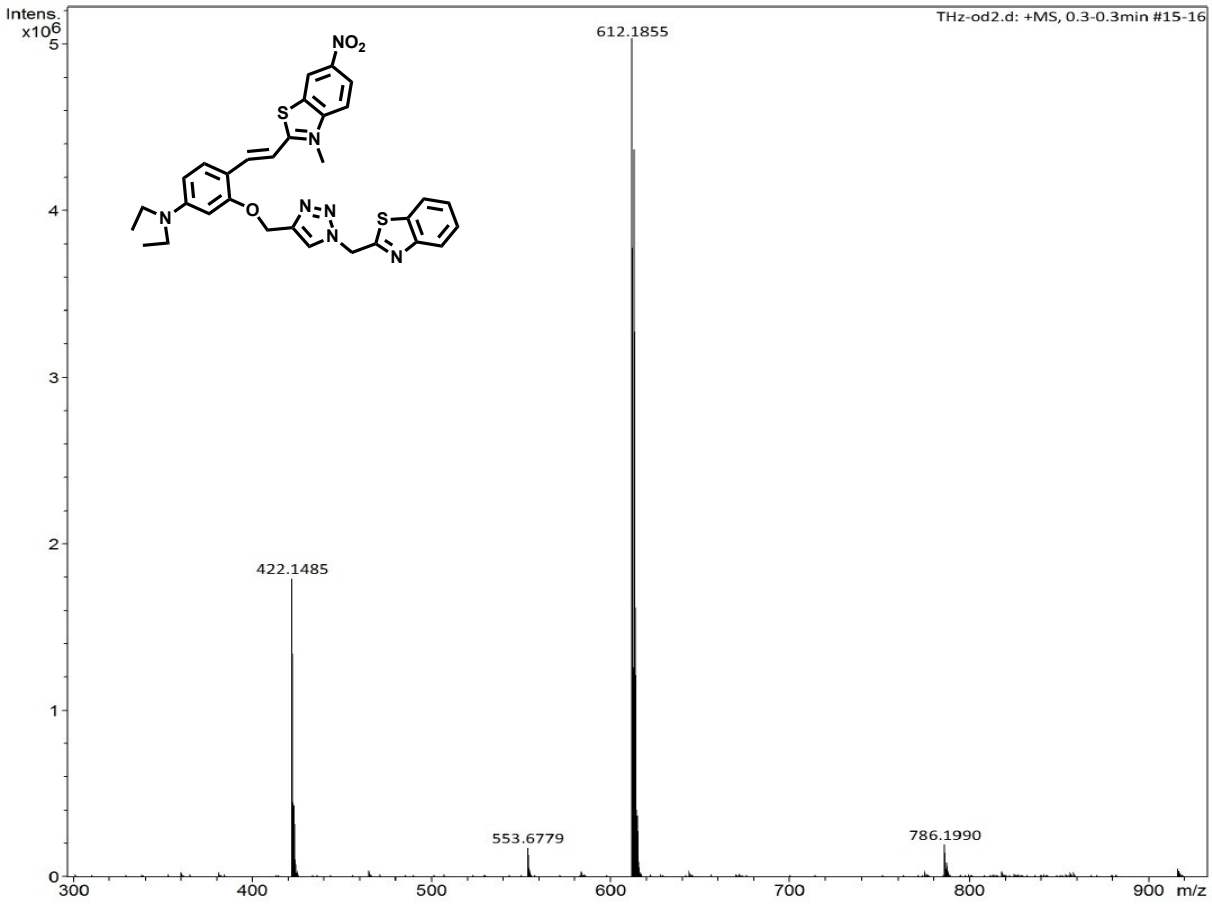
Intens.
x10^6
THz-od2.d: +MS, 0.3-0.3min #15-16
612.1855
422.1485
553.6779
786.1990
m/z

Fig. S46: HRMS

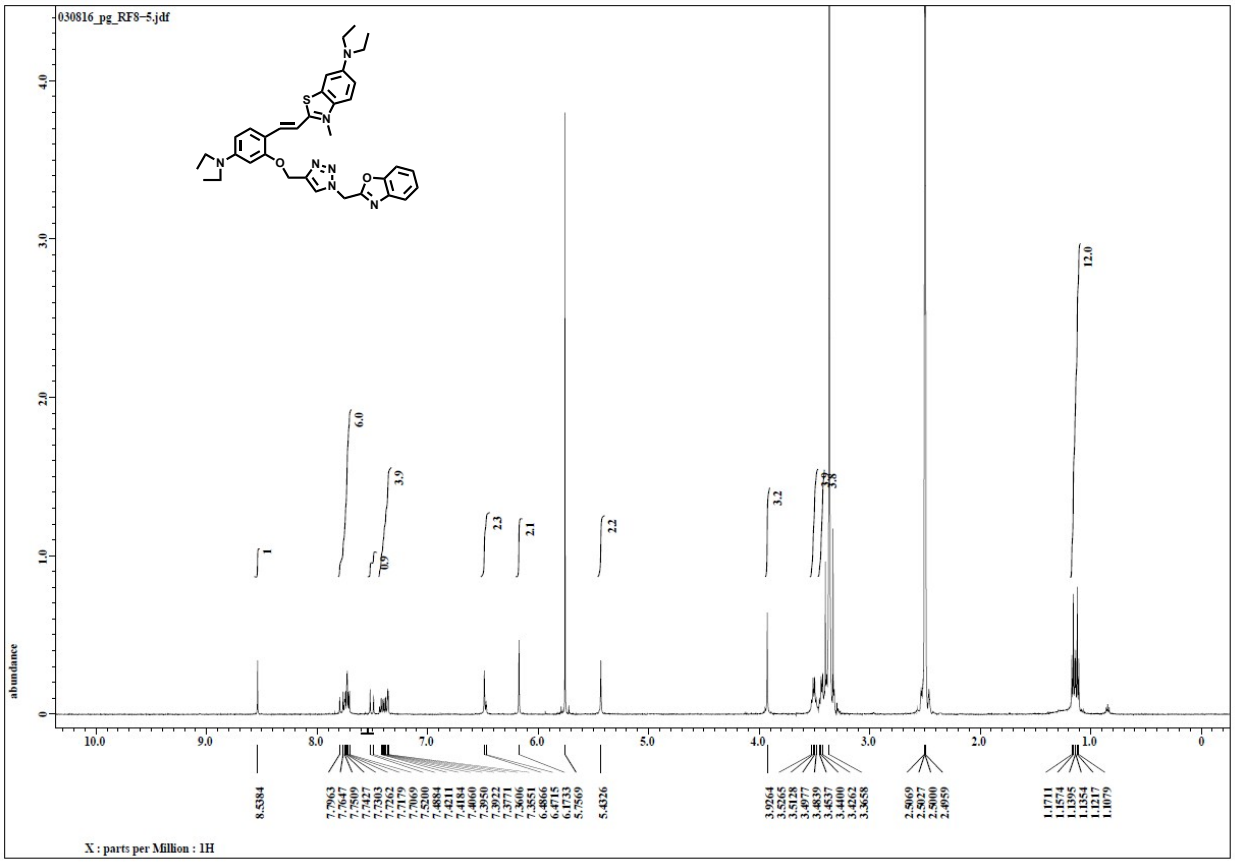

Fig. S47: ^{1}H-NMR

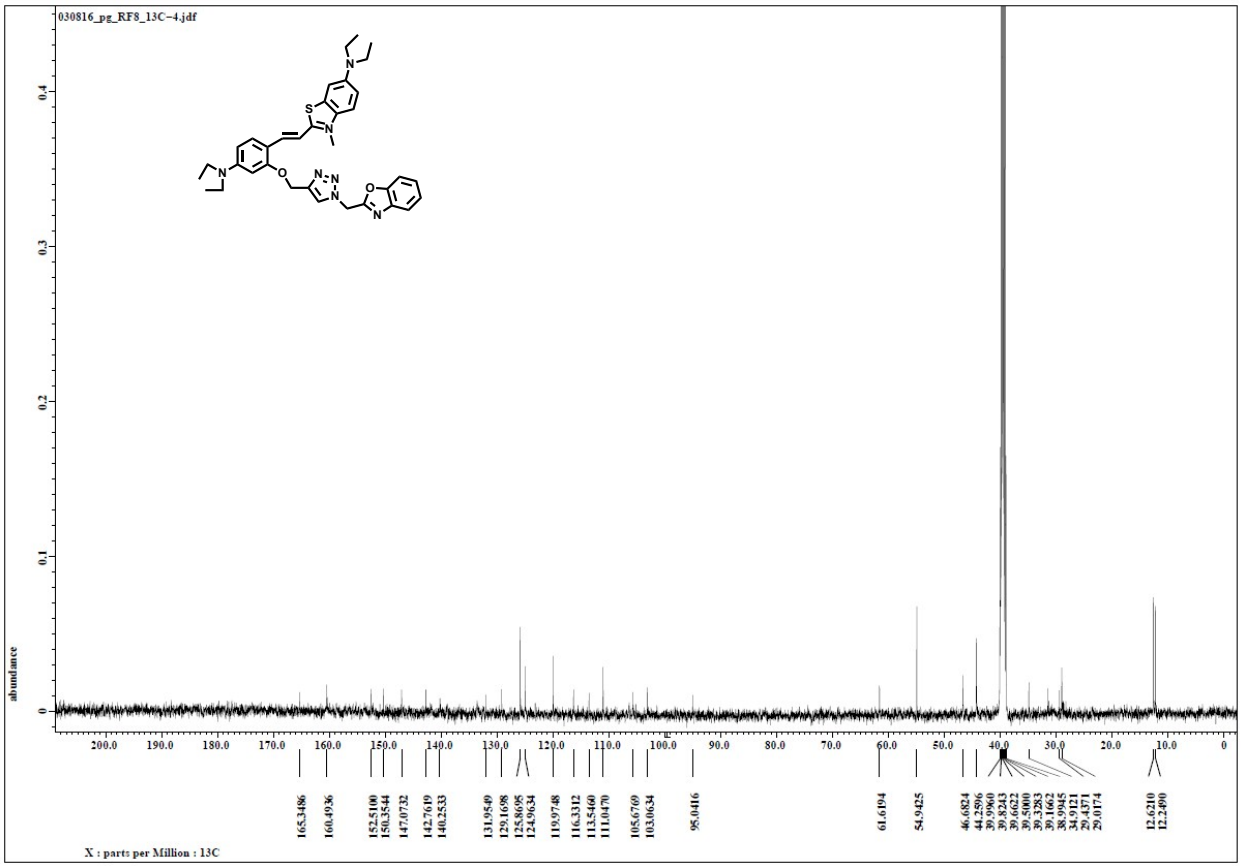

Fig. S48: ^{13}CNMR

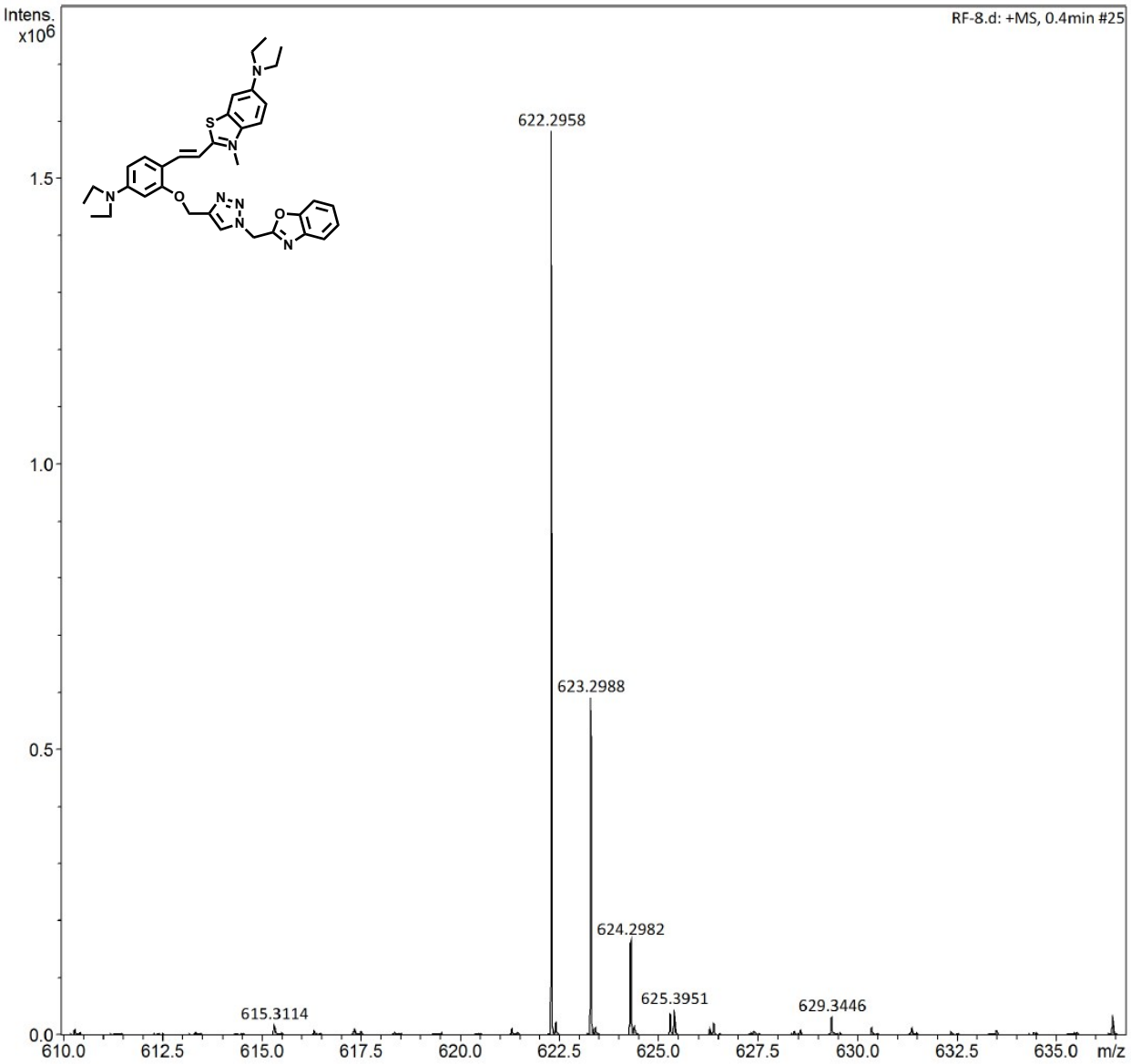
Intens.
x10^6
RF-8.d: +MS, 0.4min #25
622.2958
623.2988
624.2982
625.3951
629.3446
615.3114
1.5
1.0
0.5
0.0
610.0
612.5
615.0
617.5
620.0
622.5
625.0
627.5
630.0
632.5
635.0
m/z

Fig. S49: HRMS

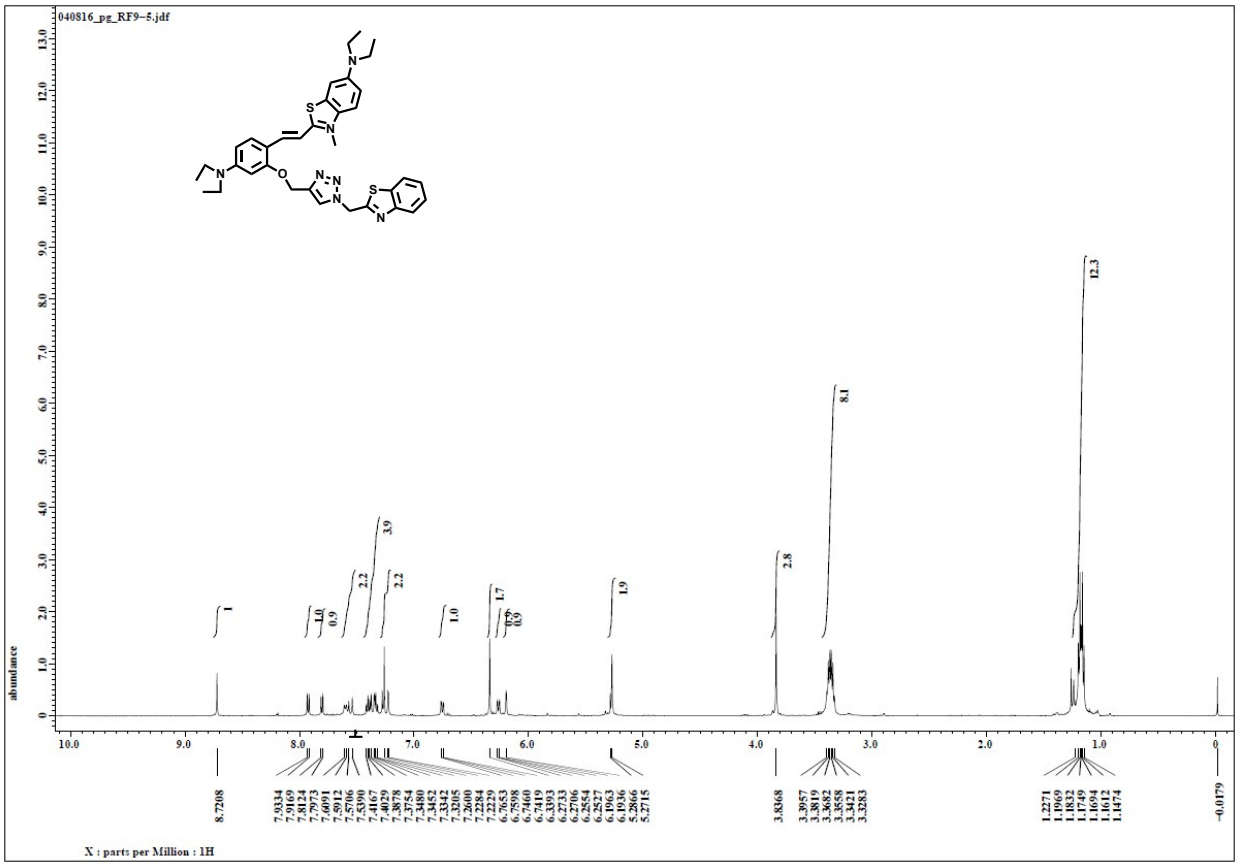

Fig. S50: ^{1}H-NMR

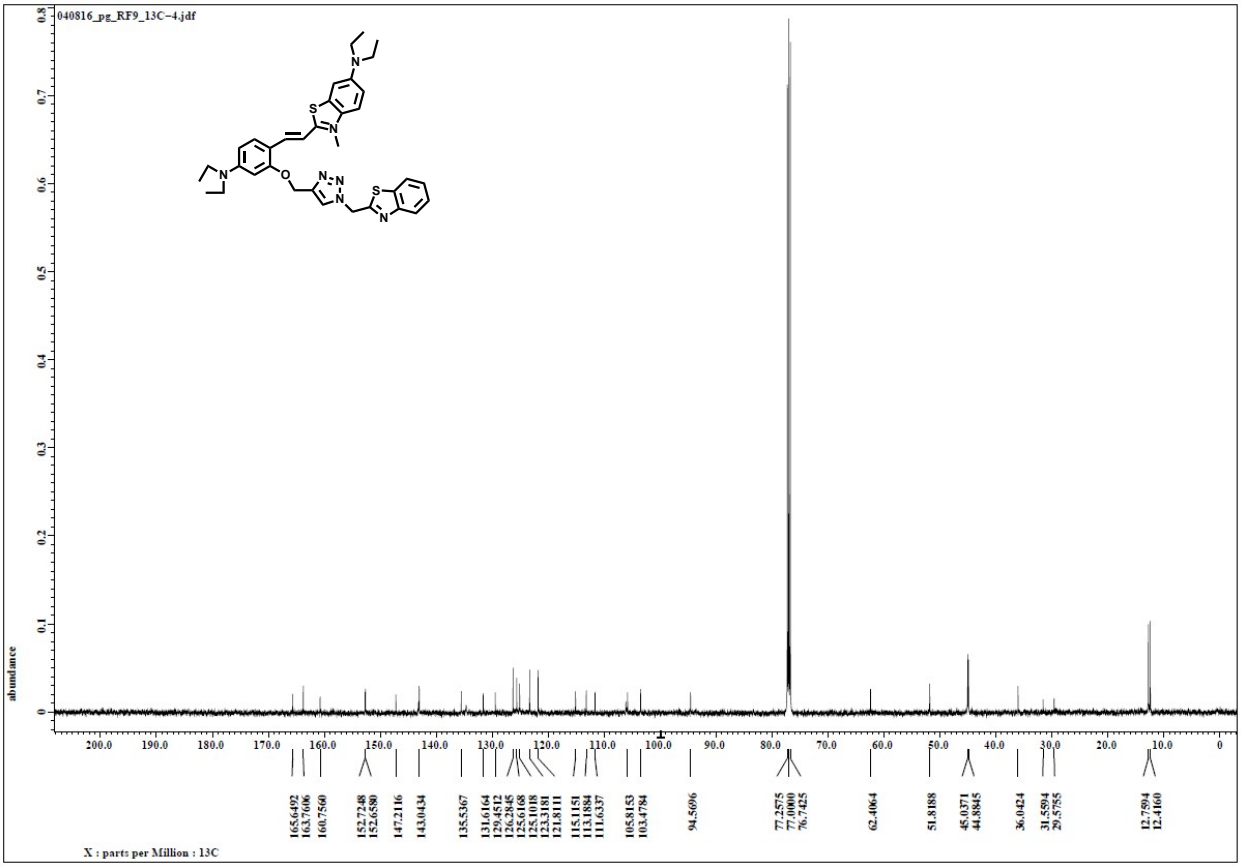

Fig. S51: ^{13}CNMR

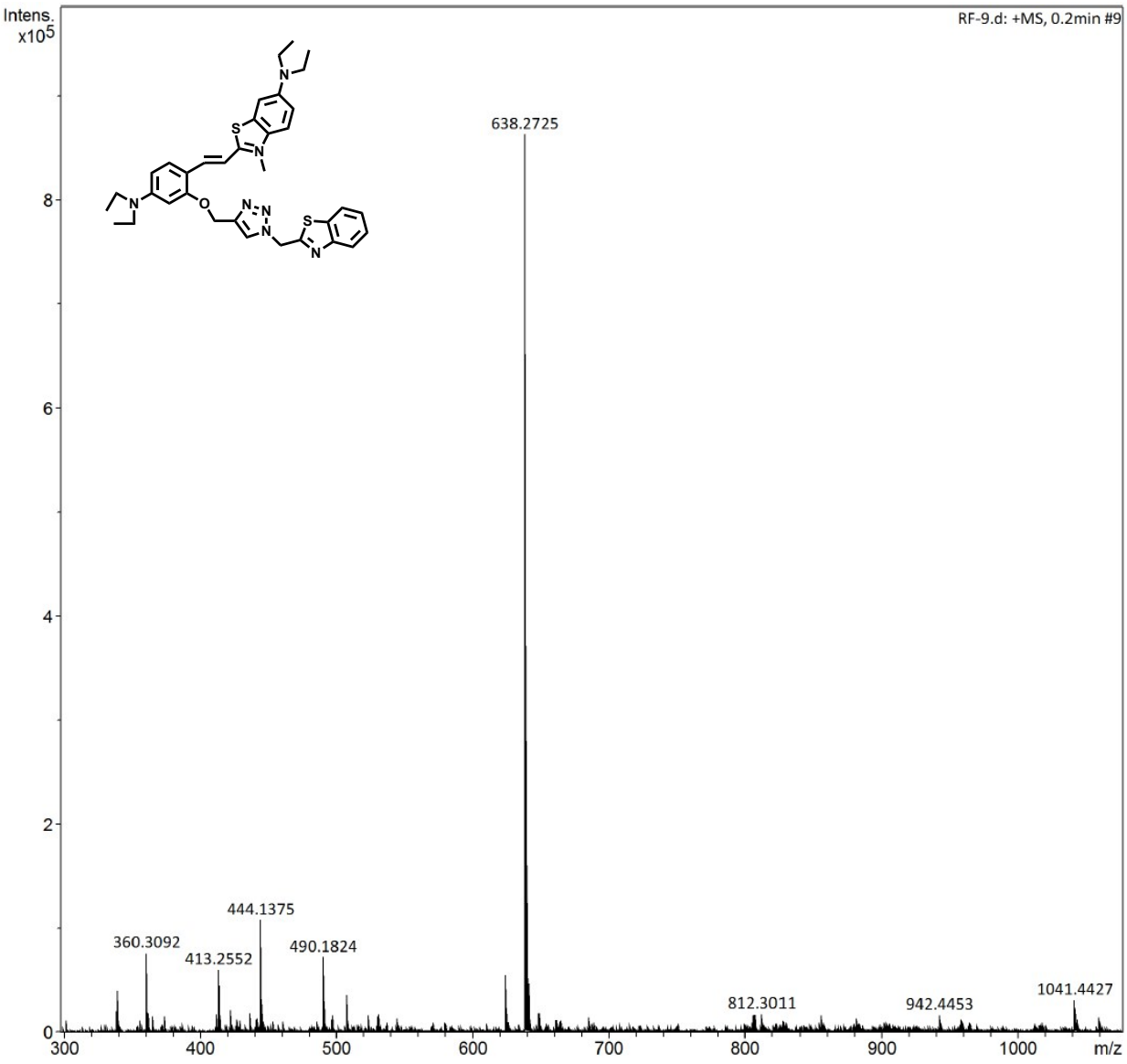
Intens.
x10^5
RF-9.d: +MS, 0.2min #9
638.2725
444.1375
360.3092
413.2552
490.1824
812.3011
942.4453
1041.4427
m/z

Fig. S52: HRMS

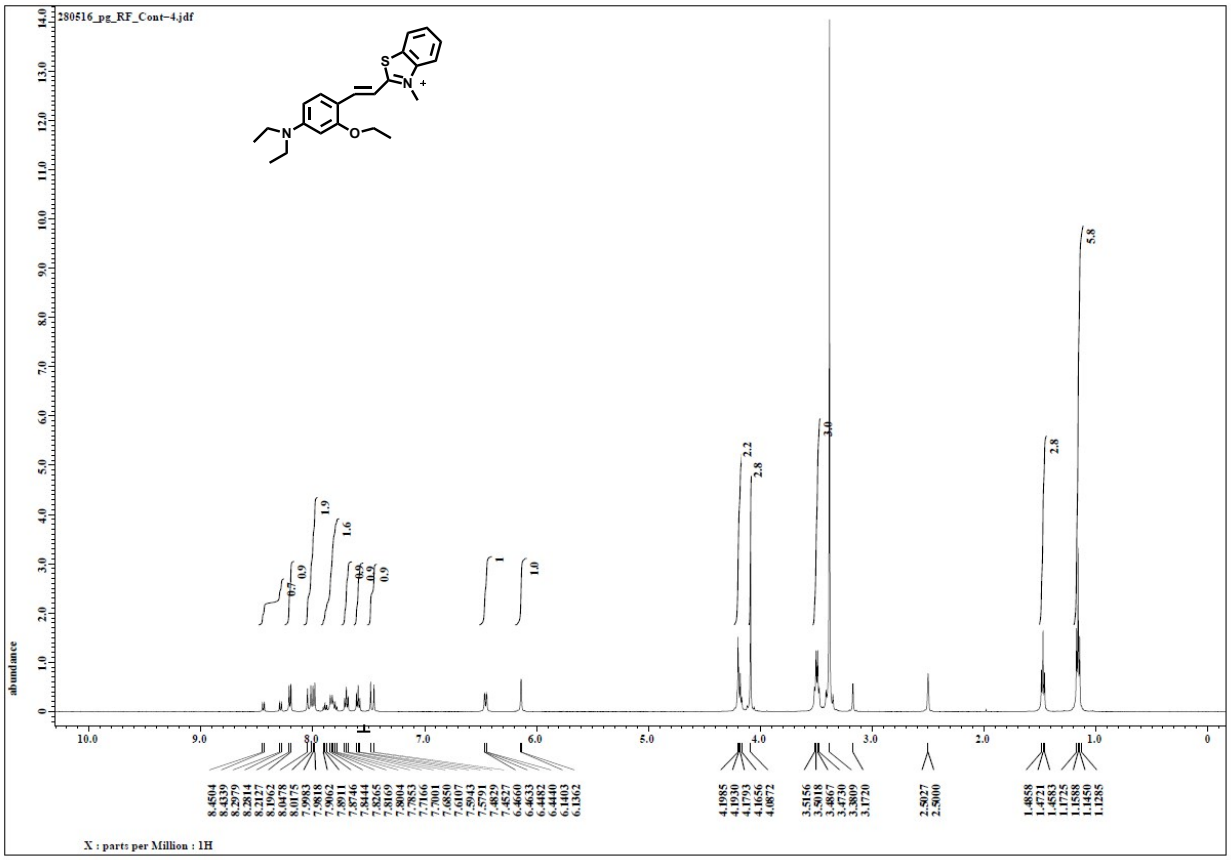

Fig. S53: ^{1}H-NMR

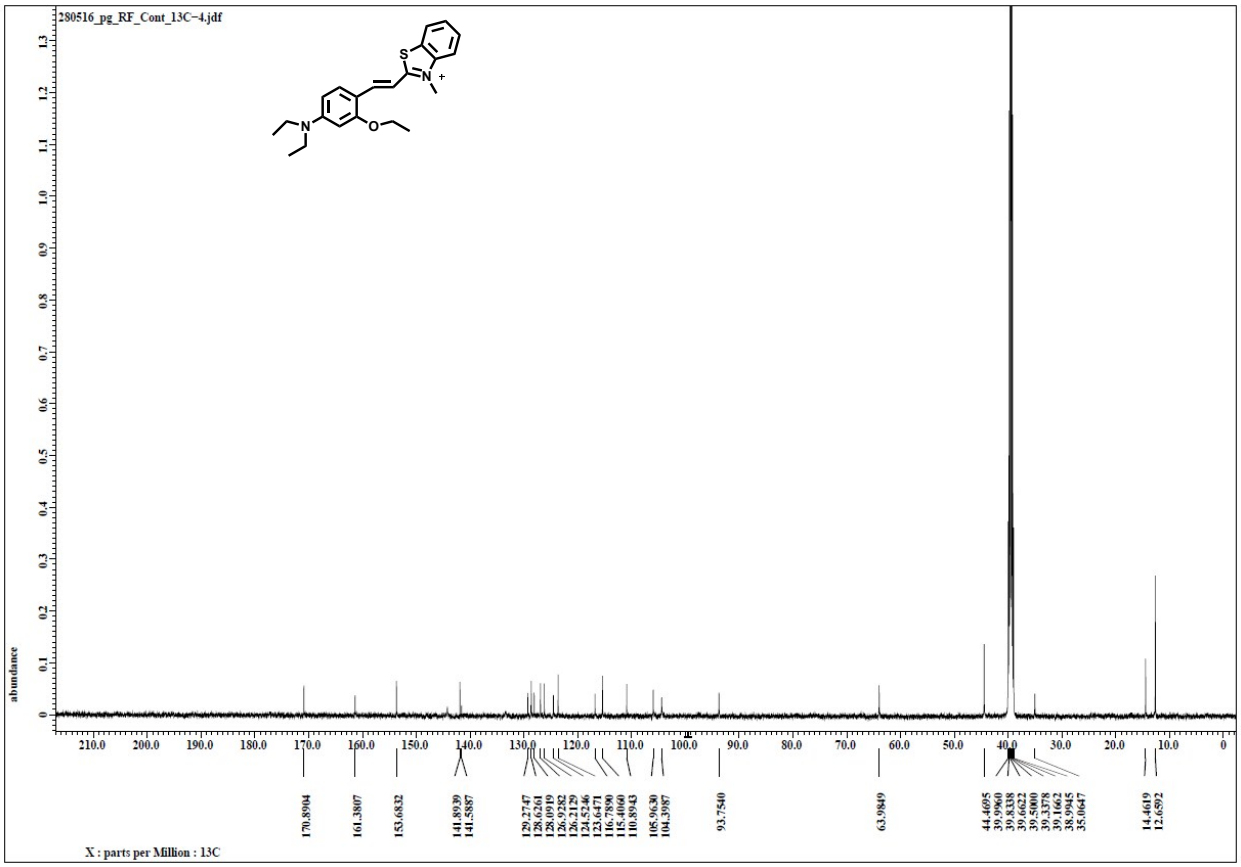

Fig. S54: ^{13}CNMR

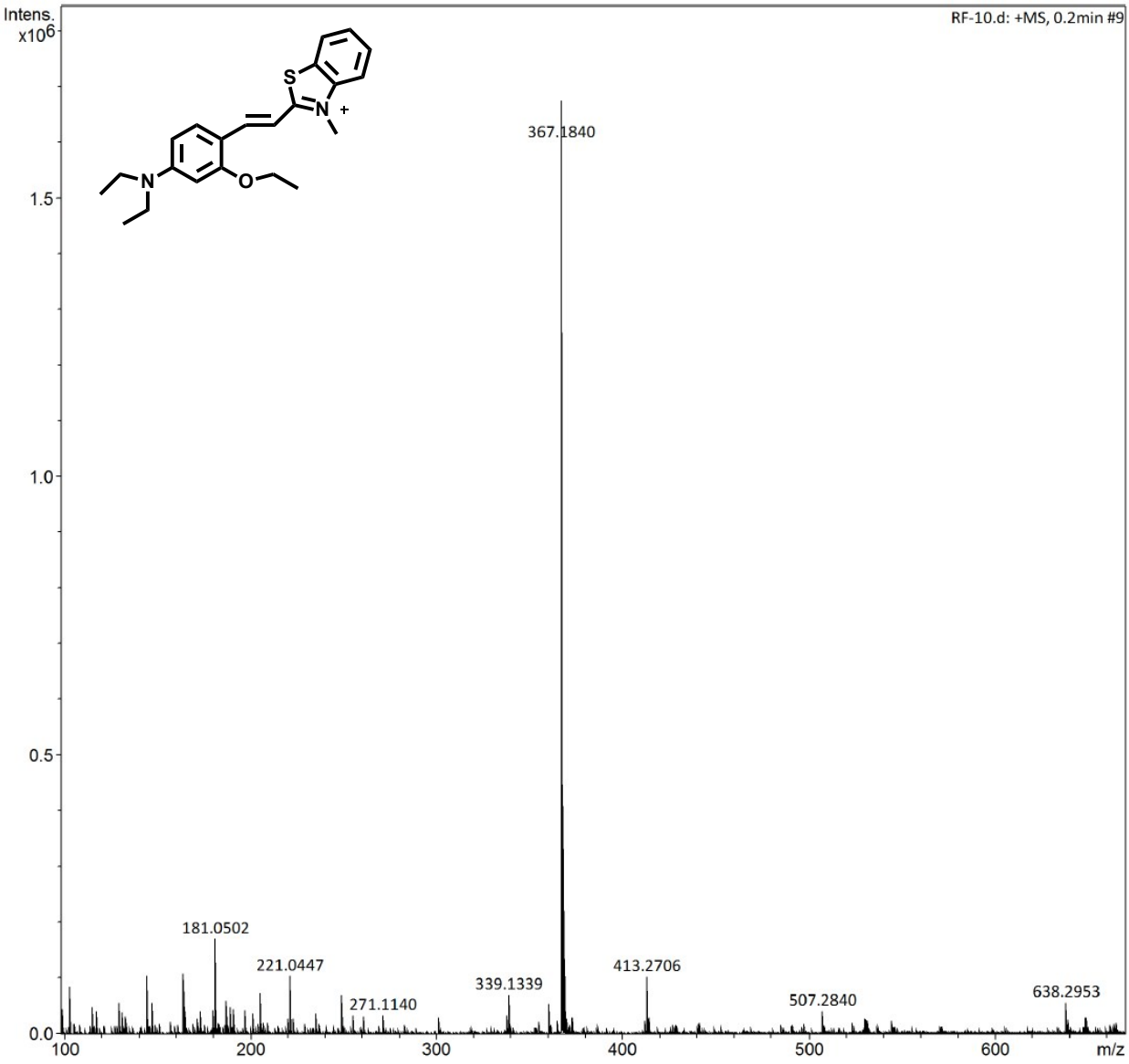
Intens.
x10^6
RF-10.d: +MS, 0.2min #9
1.5
1.0
0.5
0.0
367.1840
181.0502
221.0447
271.1140
339.1339
413.2706
507.2840
638.2953
100
200
300
400
500
600
m/z

Fig. S55: HRMS

References:

1 J. Portugal, D. J. Cashman, J. O. Trent, N. Ferrer-Miralles, T. Przewloka, I. Fokt, W. Priebe and J. B. Chaires, *J. Med. Chem*. 2005, **26**, 8209–8219.

2 A. D. Becke, *J. Chem. Phys.* 1993, **98**, 5648 −5652.

3 C. Lee, W. Yang and R. G. Parr, *Phys. Rev. B*. 1988, **37**, 785 −789.

4 M. J. Frisch *et al*., *Wallingford, CT, USA,* **2009**.

5 R. Dennington, T. Keith and J. Millam, *Semichem Inc., Shawnee Mission, KS*, **2009**.

6 P. Job, *Ann. Chim*. 1928, **9**, 113-203.

7 Y. Zhou, Z.-X. Li, S.-Q. Zang, Y.-Y. Zhu, H.-Y. Zhang, H.-W. Hou and T. C. W. Mak, *Org. Lett.* 2012, **14**, 1214-1217.

8 H. A. Benesi and J. H. Hildebrand, *J. Am. Chem. Soc.* 1949, **71**, 2703-2707.

9 B. Liu, Y. Pang, R. Bouhenni, E. Duah, S. Paruchuri and L. MacDonald, *Chem. Commun.* 2015, **51**, 11060-11063.

10 G. Dey, P. Gaur, R. Giri and S. Ghosh, *Chem. Commun*. 2016, **52**, 1887-1890.

11 C. C. Woodroofe, R. Masalha, K. R. Barnes, C. J. Frederickson and S. J. Lippard, *Chem. Biol.* 2004, **11**, 1659-1666.

12 P. R. Bohlander and H.-A. Wagenknecht, *Org. Biomol. Chem*. 2013, **11**, 7458-7462**.**

13 K. Bielawski, S. Wolczynski and A. Bielawska, *Biol. Pharm. Bull.* 2001, **24**, 704-706.

14 (a) T. Wang, M. Wang, C. Dinga and J. Fu, *Chem. Commun.* 2014, **50**, 12469-12472; (b) Y. Hao and Y. Chen, *Dyes Pigm*. 2016, **129**, 186-190; (c) A. Gellis, N. Boufatah and P. Vanelle, *Green Chem*. 2006, **8**, 483–487

15 Y. Zhang, J. Wang, P. Jia, X. Yu, H. Liu, X. Liu, N. Zhao and B. Huang, *Org. Biomol. Chem.* 2010, **8**, 4582-4588.

16 V. Hrobarikov, P. Hrobarik, P. Gajdo, I. Fitilis, M. Fakis, P. Persephonis and P. Zahradnik, *J. Org. Chem.* 2010, **75**, 3053–3068.

17 B. Chiranjeevi, B. Vinayak, T. Parsharamulu, V. S. PhaniBabu, B. Jagadeesh, B. Sridhar and M. Chandrasekharam, *Eur. J. Org. Chem*. 2014, 7839–7849

18 J. Gu, U. R. Anumala, F. Lo Monte, T. Kramer, R. Heyny von Haußen, J. Hölzer, V. Goetschy-Meyer, G. Mall, I. Hilger, C. Czech and B. Schmidt, *Bioorg. Med. Chem. Lett.* 2012, **22**, 7667-7671.

19 M. S. Mayo, X. Yu, X. Zhou, X. Feng, Y. Yamamoto and M. Bao, *Org. Lett.* 2014, **16**, 764-767.